POLITECNICO DI TORINO

DIPARTIMENTO ENERGIA

Corso di Laurea Magistrale in Ingegneria Elettrica

Tesi di Laurea Magistrale

Power-to-Gas impact on the European transmission system

Relatore:
prof. Ettore Francesco Bompard

Correlatore:
dr. Andrea Mazza

Candidato:
Antonio L'Abbate

Anno accademico 2018-2019

Table of Contents

Acronyms

AC	Alternated Current
CCGT	Combined Cycle Gas Turbine
CDF	Cumulative Distribution Function
DAM	Day Ahead Market
DCOPF	DC Optimal Power Flow
DG	Distributed Generation
DUOPF	DC Unit de-commitment Optimal Power Flow
ED	Economic Dispatch
EU ETS	European Union Emissions Trading Scheme
GA	Genetic Algorithm
GDP	Gross Domestic Product
HV	High Voltage
ID	Intra-Day
LNG	Liquid Natural Gas
LSE	Load Serving Entities
mpc	Matpower Case-file
MV	Medium Voltage
PtG	Power-to-Gas
pu	Per unit
PV	Photovoltaic
RES	Renewable Energy Sources
RPF	Reverse Power Flow
RTM	Real Time Market
ROR	Run-On-River plant (hydro power plant)
SNG	Synthetic Natural Gas
TYNDP	Ten Year Network Development Plan
UC	Unit Commitment

1 Introduction

In an effort to make technological progress environmentally sustainable, decarbonisation policies have been undertaken almost everywhere in the world with one objective: the reduction of emissions of pollutants within the limits set by well-defined scenarios. The use of energy sources from fossil fuels must be limited and consequently the larger and larger share of renewable ones, aimed at reshaping the old paradigm of energy production, must be encouraged. This transition has led to a series of technological challenges to be faced, due to the uncontrollability of these sources and the difficulty of obtaining an exact forecast of their availability. The current research direction considers the implementation of large-scale energy storage systems as a possible way to handle with these aspects. The work of this thesis, developed within the STORE&GO project framework, proposes the adoption of the Power-to-Gas technology, whose integration into the network has been analysed through two models of simulation of the Day-Ahead Market (DAM) and Real Time Market (RTM), and its consequent impact on the operation of the network. The first part of this study consists in identifying the constraints determining the amount of power of PtG units that can be installed in the network, in terms of cost and CO_2 availability. PtG costs have been evaluated accordingly to the results obtained in a previous analysis, reported in [32]: data have been interpolated to compute costs per PtG unit for a plant size equal to 100 MW and the corresponding efficiencies for the analysed scenarios. On the other hand, while CO_2 availability has been derived from [26], the corresponding maximum PtG power installable has been calculated as described in Ch.4. The investments deployed by ENTSO-E, i.e., the association of European Transmission System Operator, have been catalogued on the basis of the criteria of compatibility with the clustered grid analysed. As a result, a percentage of the budget reserved for the enhancement of the grid has been allocated to the integration of PtG technology to create one potential PtG penetration scenario. The script of the DAM model has been speeded up, through the implementation of a genetic algorithm, to allow the analysis of the network operation on four different years. Among the various possibilities, two specific analysis scenarios have been chosen:

- "**2040 Global Climate Action**" simulated with the **grid conditions related to the year *2025***, as will be presented in Ch. 5, both considering the implementation of the power-to-gas technology and without it, to highlight the positive effect on multiple indicators derived from the network;
- "**2040 Global Climate Action**" simulated under the **grid configuration forecasted for the year *2040***, without the implementation of the PtG units within the network.

The proposed comparison aims to demonstrate that the PtG technology is able to alleviate the issues affecting the network even without this being sized for the maximum load expected and to increase the quantity of RES power dispatched and thus injected into the grid.

Since the complete real data required by the model are not available for the purposes of free research, these have been obtained, as explained in the next section, combining real data with data extrapolated from analysis and statistical surveys, hence this study does not aim to provide an exact and detailed overview of the status of the European transmission network, but rather to propose a reliable methodology for the analysis and evaluation of the implementation of PtG technology in the current and future equivalent network, based on the scenarios analysed.

2 Previous results and problem characteristics

In order to face the challenges provided by the large penetration of Variable Renewable Energy Sources (VRES) innovative technologies are required, as new forms of storage to provide flexibility and robustness to the network. The project “Store&Go” addresses the exploitation of the PtG technology, proven as one of the possible solutions to the issue: it allows to absorb the excess of power of VRES generators, using the electricity to produce synthetic natural gas (SNG). As illustrated in [23], it is necessary to adopt a computational framework based on DC Optimal Power Flow, capable of simulating the day ahead market and the consequent RT market, applied to a simplified European transmission network in different scenarios of load and generation. In [23] a PtG plant model has been proposed, based on real measurements of an AEC electrolyser of 2 MW-size. Such a given PtG placement configuration results in an improvement of the system performances: to evaluate them it has been created a calculation frame built on an opensource software, Matpower, with the purpose of quantifying the effect of PtG installation in specific nodes of the grid.

Simulations have been run on the network with hourly loads, hourly average value of RES and afterwards with a 10 minute-variation being added to the average value of RES production.

The presence of PtG, as additional responsive loads, has allowed to reduce the need for reschedule, leading to a better system operation and to grid stabilization.

For the network configuration it has been used an open and updated model of the European network shown in [13] and covering all the ENTSO-E countries. This dataset groups transmission network parameters for different voltage levels and for definite types of conductor, with definite geometries. The model also permits to simplify the network, through a k-means clustering technique leading to a grid composed of 256 nodes, instead of 6000, connected via 380 kV equivalent branches. The capacity among clusters depends on the existing connections, based on the values indicated in Table 2.1.

Table 2.1: Transmission Lines Properties

Voltage [kV]	Current Limit [A]	Power Limit [MVA]
220	1290	492
300	1935	1005
380	2580	1698

Generation and load profiles, that provide information on hourly power production have also been updated according to future scenarios. In particular, loads at a country level have been distributed within the buses of each country according to their rated power per node. In addition, it has been provided a selection of future scenarios, differentiated by several features, such as forecast RES penetration and climate conditions: as a matter of fact, it is possible to choose among three load time-series representing different climatic features, i.e. dry, normal, wet, per each load scenario selected.

Regarding the generation capacity, the number of generators and their position have not been modified with respect to the network data, whereas the capacity has been scaled up. Relevant features such as minimum stable power output and the ramp rate values have been taken into consideration.

Since RES generation profiles dataset does not offer enough accuracy in terms of temporal resolution, for RTM, there is the need to adequately represent PV and wind production. Specifically, expected PV power has been estimated by gathering information on PV installed capacity from EMHIRES dataset [33] and pairing it to the one-minute irradiance values simulated by Bright's solar model [9], in order to reach a higher temporal resolution, that can be averaged according to the user's need. As well as PV, wind generation needs a higher temporal resolution. Unlike irradiance for PV, wind speed cannot be easily assumed, since it varies considerably with ground conformation, height and seasonality. Thus, it has been attempted a different approach because of the lack of wind variability information: a per unit profile has been created starting from empirical data.

The objective of the PtG integration into the grid, to act as a balancing element, has been achieved through a RT analysis based on the results of the DA optimization.

As output, the OPF provides the set of generators producing the power required to meet the system demand, at the minimum generation cost. Specifically, the day-ahead OPF dispatches the forecast value of VRES generators, typically the cheapest, and the traditional generators through an economic merit criterion, whereas the second OPF redispatches the power from traditional generation and PtG to deal with the unbalances caused by the variable nature of RES and loads as well, whose trend can be foreseen accurately but not exactly, in advance. The main goal of these two OPF is to simulate the day-ahead market and a quasi real-time market, where PtG is capable of providing its benefits to the network. While the first has a time-resolution of an hour, the latter shows a higher time-span resolution with multiple steps of hour submultiples, e.g. twelve 5 minutes time steps. The coding environment is represented by MATLAB®, recalling the OPF function implemented in Matpower.

Results showed that PtG has its deepest impact on the actual grid, the 2017 scenario, in which the installation of 10 GW (with a size per plant of 1 GW) in different nodes is able to level power imbalance of the whole network, limiting both its peak and duration. The amount of PtG power has not been varied with scenarios, with the aim of proving the feasibility of a present solution also for future outlines. RES capacity is expected to grow substantially, i.e. almost three times in the next decade, thus consequently leading to conventional generators reduce their power output. Alongside with the increase of RES availability, PtG effect on the network is more than halved as regards peak, decreasing from 50% to below 20% and around 12% for 2030 and 2040 scenarios, whereas duration reduction goes from 92% of 2017 to 48% of 2040.

These trends have paved the way for further analyses, in order to develop a more efficient PtG placement on network infrastructure and to carry out a complete investigation of its impact on the transmission system operation, within both the same scenarios and even longer-term outlines. The purpose could be served by adopting a suitable framework for solving generalized steady state electric power scheduling problems. Initially it was intended to use a specific tool included into the Matpower environment and called MOST, which is MATPOWER Optimal Scheduling Tool [34]. As a matter of fact, MOST would have been

perfectly suitable for this study, since, amongst its functionalities, it is designed for multiperiod optimal power flows, but since the current version does not handle DC lines, it was not suitable to properly represent the EU network condition.

2.1 Mathematical framework

The load flow or power flow study consists in a numerical analysis aimed at evaluating the system's capability to adequately supply the connected load. The values assumed by the variables describing the system have to be determined, i.e. voltage magnitude and phase angle at each bus, as well as current, active and reactive power flowing in each line. In addition to such information, it is possible to perform calculations to execute the unit commitment process and the economic dispatch.

Iterative methods are the essential tools for the resolution of the network. The choice of the proper method to use is based on the type of power flow to solve, which in turn depends on the type of network under analysis: for example AC power flow exploits methods as Newton-Raphson or Gauss-Siedel. Nevertheless, such methods entail a considerable computational burden, especially when applied to large and complex systems. For this reason, it is accustomed to adopting decoupled power flow methods providing approximate, but still accurate, results. The abovementioned simplification is made possible by the presence, in the transmission network, of two physical quantities responsible of the control of the active and reactive power: the former is represented by voltage angle values affecting directly the active power values, whereas the latter is the amplitude of the nodal voltages, related to reactive power. Active and reactive power flows through the lines of the network can be consequently controlled by manipulating the values of these two variables. To the extent of this study it is necessary to operate a distinction among the nodes, classifying them into three categories:

- **PV**: traditional generators are usually represented by these nodes. The physical quantities defining them are active power "P" and nodal voltage magnitude "V". These nodes are characterised by capability curves that delimitate the possible combined production of active and reactive power;

- **PQ**: this type of nodes is traditionally used to represent the passive load of the network, through active power, letter "P", and reactive power, letter "Q", that define nodes features. Recently it has also been used to describe generation nodes not taking part into voltage regulations, as for non-dispatchable generators that produce only active power P, without reactive power;

- **Slack**: in the network calculation it is assumed as reference, as a matter of fact it represents a very large generator, defined by its voltage magnitude "V" and its voltage phase angle "δ". Besides, it is also used to balance all those quantities unknown at the beginning of the process, that become known only at the end of the computation, such as network losses.

The optimal DC power flow used to solve the problem of the study is composed of a DC load flow and an economic dispatch that are computed simultaneously, explained in section 2.2 and 2.3 respectively.

2.2 Direct Current Load Flow DCLF

This method of study of network is particularly suitable for meshed network, since it allows an easier calculation of the load flow.

Hypotheses:

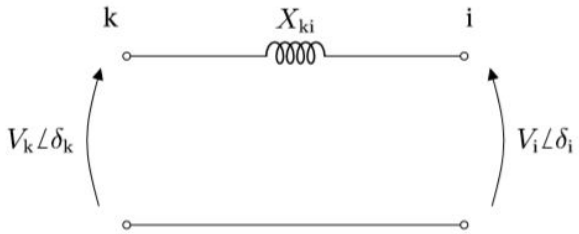

Figure 2-1. Equivalent Circuit of the line connecting two nodes

$$V_k \cong 1\ pu\ \forall k, \tag{2.1}$$

$$t_{ki} \cong 1\ pu, \tag{2.2}$$

$$|\delta_k - \delta_i| \ll 1\ pu, \tag{2.3}$$

$$R_{ki} \cong 0, \tag{2.4}$$

where *i* and *k* are nodes of the network, voltage phase angle is comparable at the two different nodes, branch resistance can be neglectable and transformer ratio is ideal, while reactive power Q_k is neglected.

Therefore, the sinusoidal AC expression indicating the power transit through a reactance

$$P_{ki} = \frac{V_k V_i}{X_{ki}} \sin(\delta_k - \delta_i) \tag{2.5}$$

becomes

$$P_{ki} \cong \frac{\delta_k - \delta_i}{X_{ki}}. \tag{2.6}$$

Thus, it is possible to operate an analogy with a DC circuit where AC quantities are associated to the corresponding DC ones.

$$\mathbf{p} \rightarrow I_{DC}$$

$$\boldsymbol{\delta} \rightarrow V_{DC}$$

$$\mathrm{X} \rightarrow R_{DC}$$

Hence,

$$P_{ki} = \frac{\delta_k - \delta_i}{X_{ki}} \tag{2.7}$$

becomes analogous to

$$I_{ki} = \frac{V_k - V_i}{R_{ki}}. \tag{2.8}$$

The slack node is here assumed as a short circuit $\delta_n = 0$ traversed by P_n, where n is the last node.

Nodal balance

$$P_k = \sum_{i=1}^{n} P_{ki} = \sum_{i=1}^{n} \frac{\delta_k - \delta_i}{X_{ki}}. \tag{2.9}$$

where P_k can be assumed as an ideal current generator injecting the power P_k to the node k.

Similarly, it is also possible to consider P_k as the sum of the power/currents flowing in the line linking nodes i and k, specifying that $P_{kk} = 0$ by definition ($\frac{1}{X_{kk}} = 0$), and $P_{ki} = 0$ whether nodes i and k are not connected ($\frac{1}{X_{ki}} = 0$).

Finally, DC power flow equations can be deduced. Given the vector of real power injection at buses:

$$\mathbf{p} = \begin{bmatrix} p_1 \\ \vdots \\ p_n \end{bmatrix}, \tag{2.10}$$

$$p_i = g_i - d_i \tag{2.11}$$

where g_i is the generated power at the bus i and d_i is the power required by the load connected at the same node.

Thus, voltage phase angles and the admittance matrix **B** are related to power injections.

$$p_i = \sum_{i=1}^{n} P_{ki} = \sum_{i=1}^{n} \frac{\delta_k - \delta_i}{X_{ki}}. \tag{2.12}$$

$$\mathbf{p} = \mathbf{B} * \boldsymbol{\delta} \tag{2.13}$$

The elements of B have been defined below.

$$\mathbf{B} = \begin{bmatrix} b_{11} & \cdots & b_{1n} \\ \vdots & \ddots & \vdots \\ b_{n1} & \cdots & b_{nn} \end{bmatrix} \qquad \begin{cases} b_{ij} = -\dfrac{1}{x_{ij}} \\ b_{ii} = \displaystyle\sum_{\substack{j=1 \\ j \neq i}}^{n} \dfrac{1}{x_{ij}} \end{cases} \tag{2.14}$$

2.3 Economic Dispatch and DC Optimal Power Flow

A lossless economic dispatch (ED) problem has the objective of finding the set of generator dispatch points that minimizes the total cost to meet the system load, without modelling network flows. The principle is that, in order to satisfy the load at a minimum total cost, the set of generators with the lowest marginal costs must be dispatched first, while the marginal cost of the final generator needed to meet the load is the one that sets the system marginal cost, i.e. the cost of delivering one additional MWh of energy in the system. This process is hence based on an economic merit criterion and its essential constraint is that the sum of the output power must equal the load demand. Another important assumption is that all the generators considered are connected to the system, this requires a Unit Commitment (UC) process to be executed first.

The UC is an optimization problem used to determine the operation schedule of the generating units that must be online, at a certain hour producing the energy required to serve the loads at the minimum operating cost. As a matter of fact, the ED could be considered a subproblem of the UC. That is, given a set of generators, divided into a number of subsets of generators, for each of the subsets of the total number of units that are to be tested, for any given set of them connected to load, the particular subset should be operated in optimum economic way [19]. This will allow to find the minimum operating cost for that subset, but it does not determine which of the subsets is actually the one minimizing the cost over a period of time. To solve this issue, a DC OPF has been chosen to obtain the global solution, whose description will follow in subsequent paragraphs.

The ED is performed through an optimization of a defined objective function. It consists of a minimization of the total cost. The objective function values are calculated over a set of decision variables subject to the constraints, that in their turn indicate restrictions on the possible values assumed by the decision variable.

According to the optimization problem general formulation, the objective function of total cost C_T is defined as follows:

$$C_T(\mathbf{p}) = C_1(P_1) + C_2(P_2) + \cdots + C_m(P_m) = \sum_{i=1}^{m} C_i(P_i). \tag{2.14}$$

The only equality constraint $h(\mathbf{p})$ to be considered at the moment is represented by

$$h(\mathbf{p}) = P_{load} - \sum_{i=1}^{n} P_i = 0. \tag{2.15}$$

Traditional calculus methods suggest using Lagrangian formulation to transform the equality constrained problem to an unconstrained one, by multiply the constraint by the Lagrange undefined multiplier λ:

$$\mathcal{L}(\mathbf{p}) = C_T(\mathbf{p}) - \lambda(P_{load} - \sum_{i=1}^{n} P_i), \tag{2.16}$$

where $\mathcal{L}$ is the Lagrange function, calculated in the optimal point P^*, in which the constraint $h(P^*) = 0$.

Therefore, at the optimal point, i.e. for the optimal dispatched power, $\mathcal{L}(P^*) = C_T(P^*)$ since $\lambda h(P^*) = 0$.

It is possible to obtain the necessary conditions for finding the optimal values of the objective function by taking the first derivative of the Lagrange function with respect to each of the independent variables and set the derivatives equal to zero. In this case there are m + 1 variables, the M values of the power output P_i plus the undetermined Lagrange multiplier λ. The derivative of the Lagrange function with respect to λ returns the constraint equation. Conversely, the M equations resulting from the partial derivative of the Lagrange function with respect to the power output values, one at a time, give the set of equations shown here:

$$\frac{\partial \mathcal{L}}{\partial P_i} = \frac{dC_i(P_i)}{dP_i} - \lambda = 0. \tag{2.17}$$

The necessary condition for the existence of a minimum cost-operating condition is that the incremental cost rates of all the units be equal to some undetermined value, λ. Besides this necessary condition, the constraint equation must be added: the sum of the power outputs must be equal to the power required by loads as shown in (2.11).

Moreover, for each of the units two inequalities constraints must be satisfied: the power output must be greater than or equal to the minimum power permitted (it depends on the generator type) and must also be less than or equal to the maximum power permitted.

$$\begin{aligned} &\frac{dC_i}{dP_i} = \lambda \quad \textit{M equations} \\ &P_{i,min} \le P_i \le P_{i,max} \quad \textit{2M inequalities} \end{aligned} \tag{2.18}$$

$$P_{load} = \sum_{i=1}^{n} P_i \quad \textit{1 constraint}$$

By introducing DC power flow equations as a function of bus voltage angle variables (see eq. (2.13)), along with limits on the branch flows, the problem becomes a DC OPF, taking into account transmission system limitations.

The objective function is analogous to the (2.16), as a matter of fact, it takes the following form:

$$\min_{\mathbf{x}} f(\mathbf{x}) = \min_{\mathbf{x}} C_T(\mathbf{x}) \tag{2.19}$$

subject to the subsequent constraints.

Since the optimization variable becomes

$$\mathbf{x} = \begin{bmatrix} \boldsymbol{\delta} \\ \mathbf{p} \end{bmatrix}, \tag{2.20}$$

both the equalities and inequalities constraints are modified as follows:

$$\begin{aligned} h(\boldsymbol{\delta}, \mathbf{P}) &= 0 \\ \delta_{i,min} \leq \delta_i &\leq \delta_{i,max}, \\ P_{i,min} \leq P_i &\leq P_{i,max}. \end{aligned} \tag{2.21}$$

The complete formulation of the DC OPF applied to the problem of the study will be presented in section 4.

3 Preliminary Work

3.1 Report on the transmission system investments up to 2040

With the aim of satisfying the energy demand of the near future, ENTSO-E planned new investments to enhance transmission network, trying to solve issues affecting the network.

These investments have been classified according to the gear of construction, for properly updating system information. Once evaluated investments effect on the improvement of the network, PtG generators are integrated, and their consequent contribution is evaluated as well. After the computation of total upgrade costs, it is assumed that a part of this capital is used to implement PtG technology into the grid.

ENTSO-E investments comprehend the construction of new lines, installation of new power stations, transformers and other equipments. The investments considered in this study have been extracted from the ENTSO-E database contained within the TYNDP 2018 [24].

This database presents the enhancement grid plan to 2025, 2030 and 2040 based on [27]:

- Pan European Market Modelling Database, from which the forecast of future network demand is derived;
- Pan European Climate Database: allowing to assess the impact of climate years within the time and resource constraints of TYNDP 2018 timelines;
- Market and Network Studies: maintenance profiles have been reported for each piece of infrastructure considered. Cross border Net Transfer Capacity calculations have been performed to evaluate limitations of each project for TYNDP 2018, in order to ensure adequate accuracy and robustness of the results with various market modelling software tools. This step guarantees network constraints not being neglected while shaping each separate transmission project.
- Cost Benefit Analysis that is essential in evaluating the total costs of the network upgrade.
- System Needs: the creation of maximum value for European citizens, the continuous access to electricity all over Europe and the compliance with objectives set out in the Climate Agenda for 2040 have been addressed.
- Frequency Stability Studies have been performed for all the synchronous areas, to ensure system's stability after the addition of new market nodes.

The TYNDP project site is equipped with a map of all the investments, carefully described with attached sheets, an example of the entire project overview is provided in fig.3-1.

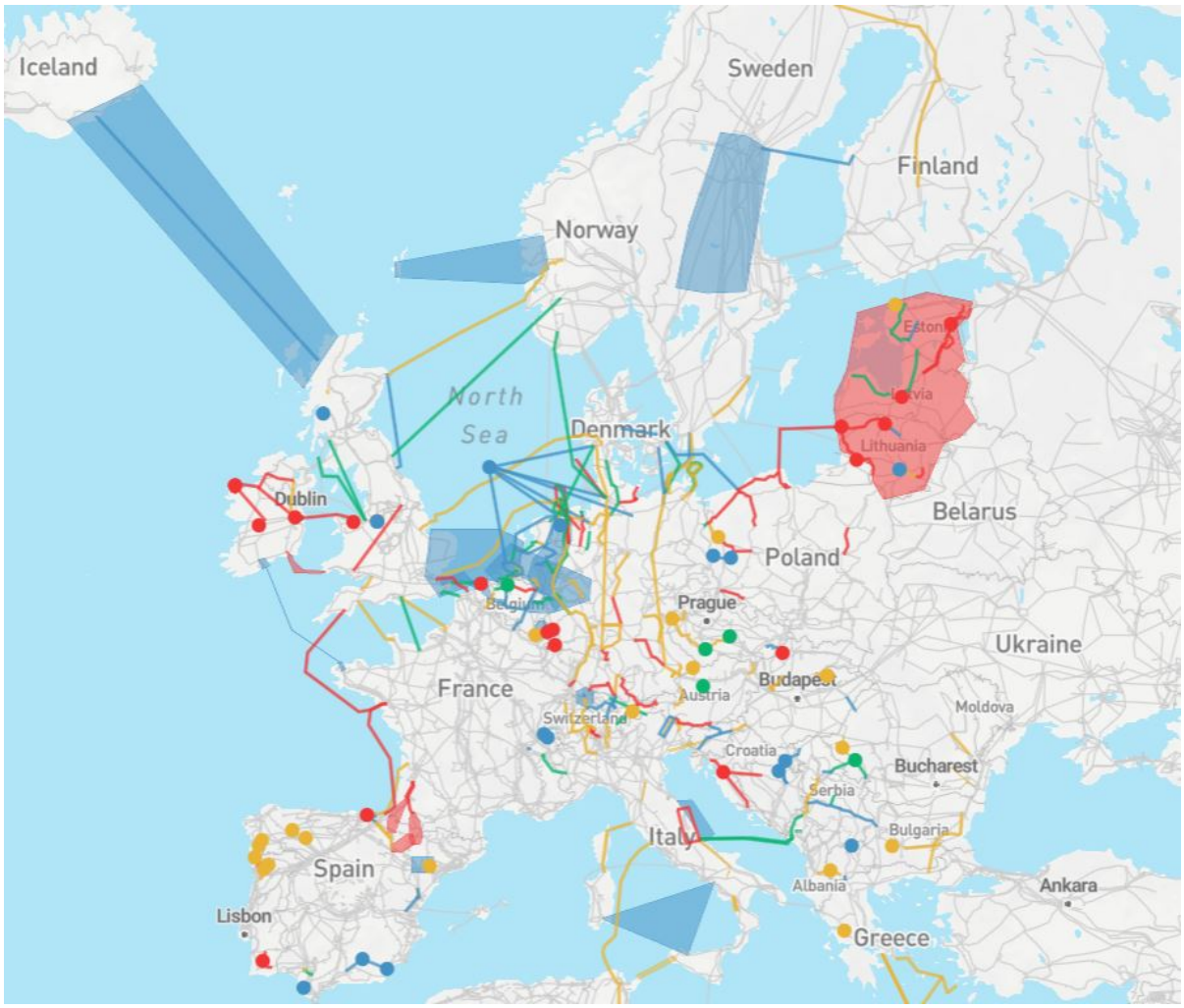

Figure 3-1. ENTSO-E's Project Map with 166 transmission and 15 storage projects. [24].

Selection criterion is based on geographical districts division, because the location of investments has been based on a map of Europe, where countries are divided into equivalent regions, the same as the ones at the basis of network clustering (Fig. 3-2).

Lines coordinates have been reported on the map to check whether their length would be contained within a region or the line connected two different regions.

Fig. 3-2. Map of Europe: equivalent regions. Visualized through www.geojson.io

Only trans-zonal investments have been considered. The adopted method is illustrated as follows:

- Coordinates of the investment (lines) have been reported on map to identify starting point and final point in order to visualize its position with respect to regions borders;
- If trans-zonal, the investment is relevant and thus included in the list.
- Data of interest are: ID project and name, costs of the project, i.e. CAPEX and OPEX, length (in km), voltage level, type of the connection, starting and final points, capacity increase (measured in MW), status of the project, commissioning year and evolution driver.

A time sorting has been applied to the list with the purpose of creating three scenarios of the grid.

- 1st from present to 2025 and indicated as 2025 scenario;
- 2nd from 2026 to 2030 and indicated as 2030 scenario;
- 3rd from 2031 to 2040 and indicated as 2040 scenario.

There are no further data available post 2040 from ENTSO-E TYNDP [29], which provides a detailed overview of the possible evolution of the European transmission network. The summary of the investments are shown in Table 3-1, Table 3-2 and Table 3-3.

Table 3-1: Scenario 2025 Investments

	CAPEX [M€$_{2018}$]	OPEX [M€$_{2018}$]
TOTAL 2025	59699.44	544.8322

Table 3-2: Scenario 2030 Investments

	CAPEX [M€$_{2018}$]	OPEX [M€$_{2018}$]
TOTAL 2025-2030	13937.98	76.967
TOTAL 2030	73637.42	621.7992

Table 3-3: Scenario 2040 Investments

	CAPEX [M€$_{2018}$]	OPEX [M€$_{2018}$]
TOTAL 2030-2040	2043.14	25.7605
TOTAL 2040	75680.56	647.5597

3.2 Potential emissions of CO_2 to be used for PtG plants

The placement of the PtG units in the grid is highly dependent on the amount of CO_2 available in the surrounding area. In fact, the CO_2 availability affects the methanation step The first step of energy conversion consists of the production of hydrogen from renewable electrical energy, thanks to the electrolysis process: water molecules dissociate within the electrolyser stacks. The second step is represented by the subsequent synthesis of methane. The methanation unit consumes carbon dioxide (CO_2) captured from flue gas streams or ambient air during the methanation process, delivering Synthetic Natural Gas (SNG or CH_4). The current research direction is to explore the possibility of capturing CO_2 both from free air and from industries. Certain industries cannot avoid emitting CO_2 as by-

products from their production processes, thus a technology that permits to contain and leverage these emissions is to play a key role in the future energy transition.

The objective is to obtain the total amount of CO_2 available per country, in order to convert these values to electrical power that is possible to derive from PtG units operation. As reported in [32], the theoretical regional potentials for SNG production have been evaluated by correlating European datasets on carbon dioxide emissions with geospatial data on RES energy generation sites. The potential carbon dioxide available per country has been calculated by industry sector, and consequently potential methane quantities have been derived. Data evaluation has been based on the E-PRTR [35] that provides data from industry sectors from the 33 European countries upon which the clustered grid is based.

For the identification of the potential PtG sites, the precise locations of biogas plants, industries emitters of carbon dioxide have been necessarily taken into account. Data are mostly made of coordinates, maps with marked plants and addresses, thus geocoding and geo-referencing have been required to make the database homogenous.

As additional step, wind farms locations across all over Europe have been mapped, because of the need for PtG units to be supplied from VRES. In particular, wind turbines allow PtG to operate also at night, hence increasing its operation time, besides being widely diffused across the continent: wind installed capacity represents more than 11.6% of EU's electricity demand. Coupling with PtG technology is obviously possible also for other regenerative energy sources, as hydro, solar, etc…, despite expectable number of full load hours being smaller, which directly affects methane production costs.

The countries exhibiting the highest potential for PtG are Germany and United Kingdom, that hold the highest amount of installed capacity of wind and biogas plants. The same analysis has been conducted on the latter plants and other biological CO_2 sources, indicating a wider distribution among the other countries. As a matter of fact, it is expected that bioenergy production will be increased in all the member states, consequently leading to a rise in potential for PtG (methane) energy conversion based on biogas.

Starting from both the results of research [26] and databases data, a comparison between the equivalent availability of CO_2 per country, computed as the sum of the availability of the clusters, and the corresponding measured values has been performed. Once computed the difference, the same has been done with the equivalent and real per cluster (node) CO_2 values, that have been levelled: the difference has been redistributed proportionally to the internal clusters of the countries.

These values have been consequently converted into maximum installable capacity of PtG units per node, through the following expressions:

$$CO_2 mass = \frac{H_2 mass * MM_{CO_2}}{4 * MM_{H_2}} \tag{3.1}$$

where the quantity of CO_2 is calculated by multiplying hydrogen mass by the CO_2 molar mass and dividing all by the hydrogen molecular mass and the stoichiometric factor 4.

It is now useful to provide the correlation between hydrogen mass and the rated power of the electrolyser installed into the PtG plant:

$$H_2 mass = \frac{P_{el}^{nom} * \eta_{Ptg,type} * f_u}{LHV_{H_2}[\frac{MJ}{g}]} \ [MJ] \tag{3.2}$$

where LHV_{H_2} is hydrogen's lower heating value, $\eta_{Ptg,type}$ is the efficiency of the technology and f_u is the utilization factor of the plant, assumed equal to 0.6 to be multiplied for the number of seconds in a year (8760 h * 3600 s) and expressing the hours of actual operation of the plant.

By substituting (3.2) in (3.1), the rated power of the plant can be derived from the available CO_2, assuming that it can be entirely used for power production.

$$P_{el}^{nom}[MW] = \frac{1}{2} \ CO_2 mass \ [g] * 4 * MM_{H_2} * \frac{LHV_{H_2}}{\eta_{Ptg,type} * f_u * MM_{CO_2}} \tag{3.3}$$

where it is assumed that only 50% of the available CO_2 is captured.

With the completion of the described procedure, all the constraints necessary to the implementation of the PtG technology into the grid have been defined, except for the cost, since the binding CO_2 values have been determined, while investments costs have been analysed in the previous section. The total quantity of PtG power that is possible to install into the grid is strictly related to the cost of the plants and the budget available. The costs have been reported in the table below, while regarding the budget it has been assumed to allocate an amount that is equal to the one destined for grid enhancement from 2025 to 2040, i.e. nearly 16 billion of $€_{2018}$.

Table 3-4: PtG unit costs

	PEMEC- CAT	**AEC-CAT**
	Cost per 100 MW unit [M$€_{2018}$]	Cost per 100 MW unit [M$€_{2018}$]
2020	222.8	227.3
2025	164.8	185.85
2030	106.8	144.4
2040	80.15	110.7
2050	53.5	77

The quantity of PtG power that will be inserted into the Ch.5 simulations is derived by averaging the costs of the two technologies considered for 2040 and assuming that each PtG unit has a size of 100 MW. If the cost of a unit is 95 $M€_{2018}$, then it is possible to install 16.85 GW of PtG.

4 Improvement of the code for day-ahead market

4.1 DAM and RTM

The purpose of this section is to describe the solutions developed to solve the critical issues of the algorithm presented in [23] and in [20].

In order to analyse the code and compare it to the new version, it is particularly appropriate to contextualize what the scripts represent: mostly because they are named after the DAM and the RTM.

DAM and RTM were created after the deregulation of the electrical systems to foster the competition in electricity generation, to consequently increase efficiency and to lower the electricity price by performing trading transactions of energy sale and purchase. Because of the features of power generation, transmission and consumption, i.e. the need to produce the exact quantity of demanded power due to non-storability in large scale, there is a trading session opened days before consumption, in which most of the sales and purchases are hosted. Besides, there are multiple sessions during the reference day to ensure that unbalances between forecast and actual load demand as well as VRES generation's are corrected, thanks to the adjustments to generators output power.

The DAM is thus responsible of the generation and demand scheduling and prices for the following day through an auctioning process, in which hourly energy blocks are traded. The mechanism behind this market is simple: starting from TSOs preliminary information about hourly energy demand, renewable programs and network constraint, generation suppliers sell their energy production packages through offers with the format price-quantity, specifying the quantity and the minimum price at which they are willing to sell. On the other hand, Load Serving Entities (LSE) buy energy in advance, predetermining the quantity of energy needed to meet the demand of the following day and bidding price/quantity offers in the market, that express their willingness to buy. Each zone or bidding area in the European Power System has its own Power eXchange collecting participants orders. Once electricity orders have been proved feasible, from a technical/security perspective, they are accepted, otherwise rejected: price is given by the intercept of supply and demand curves and in Italy is calculated as PUN (Prezzo Unico Nazionale, i.e. Unique National Price).

Regarding RTM, trading mechanisms are similar to DAM ones: buyers and sellers make their offers/bids according to day-ahead results and to the related real time deviations. These deviations can be caused by multiple reasons: from unexpected outages, to weather variability causing renewable generators to produce at different power output than previously estimated. Currently, this market settles only a minor part of the produced energy, but as VRES diffusion increases, it is becoming more and more important, due to the need for its balancing action. In addition, it can play as key enabler to increase the share of renewable energy in the energy mix. Real time trading makes this market continuous, as transactions takes place every day in seven sessions (Italy), distributed both in the day ahead and in the day of the consumption, with a time span resolution higher than hour, usually 5 minutes [16]. Supply offers and demand bids are selected under the same criterion as for the DAM, although being paid at the zonal price when congestions arise.

4.2 Scripts features

The algorithms created in [20] and [23] to simulate the abovementioned markets is made of two different parts, running two optimizations:

- the first one, that is based on the expected values of load and generation;
- the second one based on the actual values of PV and wind generation, that emulates a real time market.

To figure out the proper placement of the PtG units it is necessary to compare the markets outputs, hence evaluating the RES variability impact on the electrical system as well as PtG impact.

These scripts have been developed within the Matpower environment and due to this fact, all input data have been adapted to the program structure (i.e. the *mpc* file). Accordingly, the results are presented with the same format, which it has been extremely convenient for creating a multiperiod problem solver code, starting from a steady state network output. Input data have also been endowed with additional information about generators type and bus country, in order to ease data sorting and filtering in the algorithm execution, without interfering with the program functionalities. Power flows are easily executable into the algorithm because of the implemented matpower functions require only *mpc* data as input.

The crucial part of the DAM script lies in the economic evaluation of the OPF calculation: every generator indicated as available for UC is considered online by Matpower and kept operating at its minimum stable power, thus increasing the cost for the network. With the objective of diminishing total costs, Matpower provides a Unit De-commitment algorithm turning off the most expensive generators. This step is the most sensitive as concerns computational time, consequently, other measures have been taken in order to simplify and speed up the algorithm: optimal DC power flow has been adopted to serve the purpose. In fact, it allows to manage production levels by generators costs and limits, internally included in the input data, leaving only ramp limits to be externally set. Such settings give the possibility not to provide generation profiles for traditional generators, whose output is set by the market logic.

Before presenting a detailed description of the DAM and RTM algorithms it is necessary to highlight the mpc main features, containing all the network parameters required for the OPF execution:

- Buses: load value, location and voltage values;
- AC lines: nodes at the extreme of lines, capacity, number of equivalent lines in parallel;
- Generators: type, status, size, ramp power variations (up and down), location, marginal cost, minimum and maximum power;
- DC lines: nodes at the extreme of lines, capacity.

Due to the fact that Matpower is able to solve only steady state problems and not time-evolving ones, other variables have been created to store time related data, as to load them at each iteration into the *mpc*. Time-dependency has been added through an external loop, allowing to perform calculations on the basis of the results of the previous step. Load and

renewable generators profiles are loaded from *-mat* files, the latter of which have been created on purpose to be adjusted to the problem nature, i.e. higher temporal resolution. While PV profiles have been loaded by accessing them directly from hard drive because of their size, wind profiles are instead calculated on the go by the algorithm. Hourly average wind profiles and clusters of variance are loaded and then, once the probability weights have been applied, the variance profile is extracted for each value of average profiles and for each wind generator and thus applied on its turn to average hourly profiles. PtG profiles have been created on the basis of network stabilization: in order to being able to vary the units production levels of the same quantity both upwards and downwards and assuming a minimum power of 20% of rated power, the reference value has been set to 60% to give the possibility of reaching the maximum power.

4.2.1 DAM algorithm

The DAM algorithm is structered as a loop, in which the iterations represent hours.

For each iteration:

- A function updates time and all time-dependant variables, as nodal loads, current PV and wind generation forecasts;
- A DUOPF is performed to generate a list of generators that need to be online for optimally supplying loads in that iteration, without violating generators or branches constrain;
- The list of essential generators is saved and assigned to the current hour;
- RES variable nature causes deviations from expected output power to be corrected in the RTM. For this reason it is necessary to have additional generators online, in order to provide both security, reserve and ramp services. These extra generators[1] are chosen among the cheapest that could not take part into the day-ahead market and the corresponding added capacity depends on seasonality and time;
- After this addition, the DCOPF is performed to clear the market in the current operation. Output is hence saved and as current iteration ends, the successive begins.

When all the hours of the selected day have been processed, the DAM loop algorithm ends.

The DUOPF step represents a severe limitation to the script use for simulating long periods and relegating it to be adopted only for single days. The reason for the eccessive amount of time required for it to be executed lies in the poor performances given by the deterministic algorithm implemented in Matpower. It considers the cost of keeping online generators working at their minimum stable working point, also in the OPF evaluation. The basic deterministic routine modifies generators' status with a logic comparable to the branch exchange method and it is not advised as number of generators increases, because of the rapid growth of the computational time required. In order to soften the resulting limitation, the original deterministic logic has been modified to include a basic heuristic that excludes some of the most expensive generators operating at the minimum power, by reducing computational time of a factor three.

[1] Additional generators are necessary at sunrise and at sunset because of steep variations of irradiance in PV production, thus urging the need for ramp service.

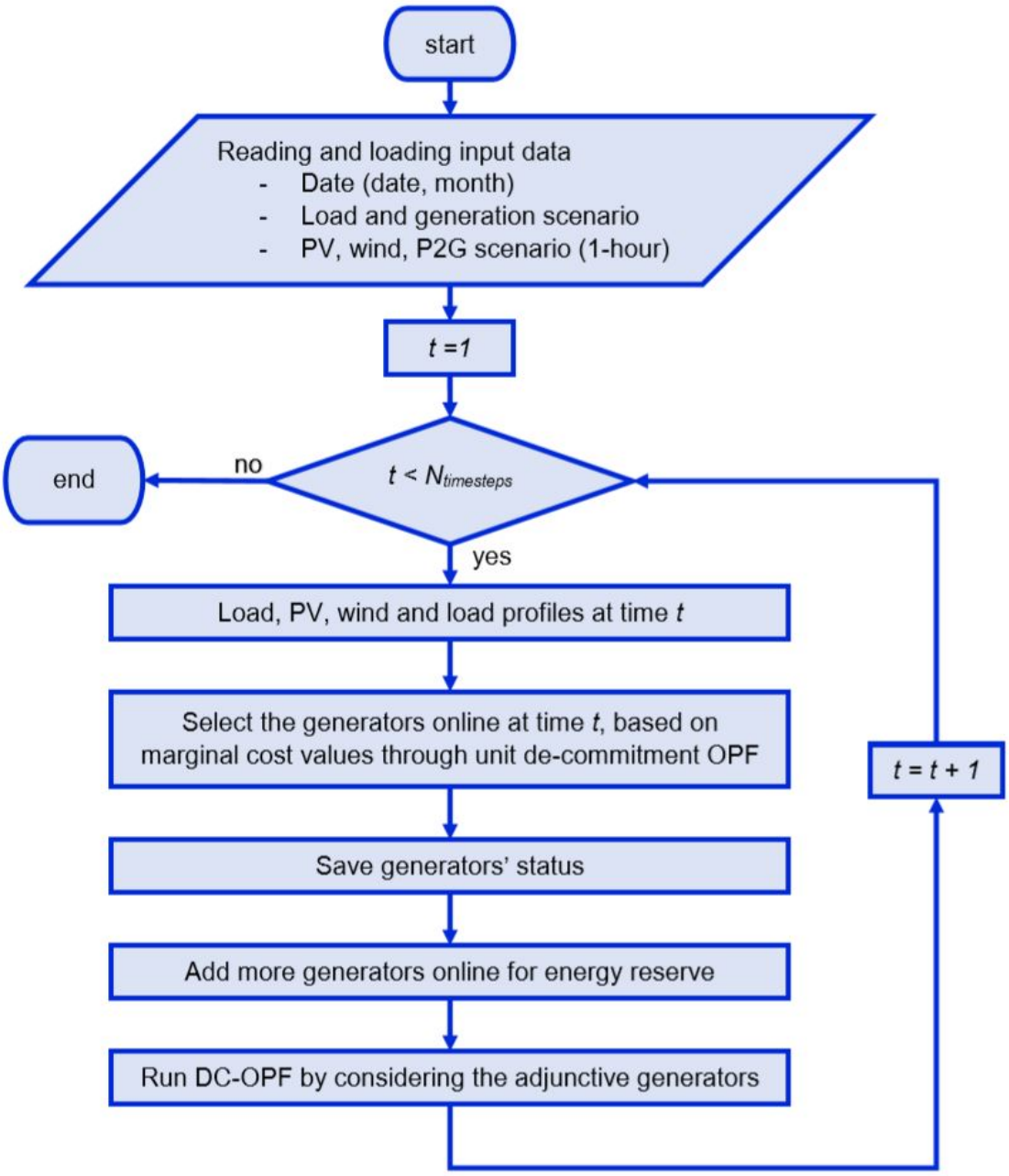

Figure 4-2. DAM flow chart [23].

The binding restriction on computational time has led to adopting a new method of analysis for the network in this dissertation. In the beginning, rather than using Matpower, it had been chosen MOST, the advanced tool supplied with Matpower, specifically designed for multiperiod electric problems, as the one of this study.

MOST approach consists of duplicating the single period problem for each period belonging to the planning horizon and combining them all into a single large problem, where individual periods appear as islands in a single network. The connection between adjacent periods is represented by ramping costs and constraints involving the corresponding dispatch variables.

Because of the possibility of addressing also problems with discrete unit commitment decisions, MOST represents the solution to the computational time issue of the DUOPF

algorithm. As a matter of fact, generators are not considered online altogether from the beginning in the economic evaluation, on the contrary optional start-up and shutdown costs are associable with changes in online status in a prior commitment state: in other words, only the generators the optimize the total network cost are committed to serve the load, hence there is no need of a Unit De-commitment process. This crucial feature allows to run the day ahead OPF on the network of the study in less than 600 seconds, the implication is straightforward: it is possible to perform a DAM of a whole week in barely more than one hour. The difficult custom implementation of DC lines into MOST script has led to a different approach, once again: a genetic algorithm has been developed to speed up the original MATPOWER based script. The deterministic algorithm has been entirely substituted, so that the Unit De-commitment process could be handled solely by the genetic heuristics. As later described in Sec. 4.4, this specific enhancement to [23] code has led to even better results than originally promised by MOST simulations, because computational time has been reduced to 4 minutes per day, hence allowing to run monthly simulations in almost 2 hours, which is the amount of time originally required to perform a single-day simulation.

4.2.2 RTM algorithm

As previously explained, the real time script is subsequent to the day ahead one, since real time market is based on the day ahead market results, which act as input: the expected power dispatch of the generators with output power levels, their prices and UC commitment schedules. It is composed of an hourly time loop, whose task is to update time-varying variables, and an inner loop, within each hour cycle, representing the user defined time steps.

PV and wind profiles are updated inside the RTM loop, averaged according to the user time step. The difference between actual renewable power produced and expected one, set in the day ahead market, is calculated per each PV and wind generator. PtG generators, in their turn, are able to exploit part of this power deviation from forecast levels: if the difference is positive, there is more VRES availability than expected, hence the setpoint at which PtG units work represents an absorption of power, otherwise it means that they need to lower their uptake to help the network, because there is a lack of power generation with respect to forecasts. As soon as PtG setpoints are established, for the current RT step, PtG model is run for each unit. The outputs of the models represent the response of the units in the current minute (there is a higher temporal resolution available): translating into Matpower modelling this means that responses are equivalent to load values of the dispatchable loads. Ramp constraints are enforced through maximum and minimum power of the generators. At the beginning of each iteration, generation results of the previous step are taken into account, thus maximum and minimum power constraints are updated as follows: ramp rates are applied to the user defined time step for the RTM and added or subtracted to the previous results values. Finally, a DCOPF is performed, the related output is hence saved for the current iteration and the loop starts again with a new iteration, otherwise ends, if the iteration is the last.

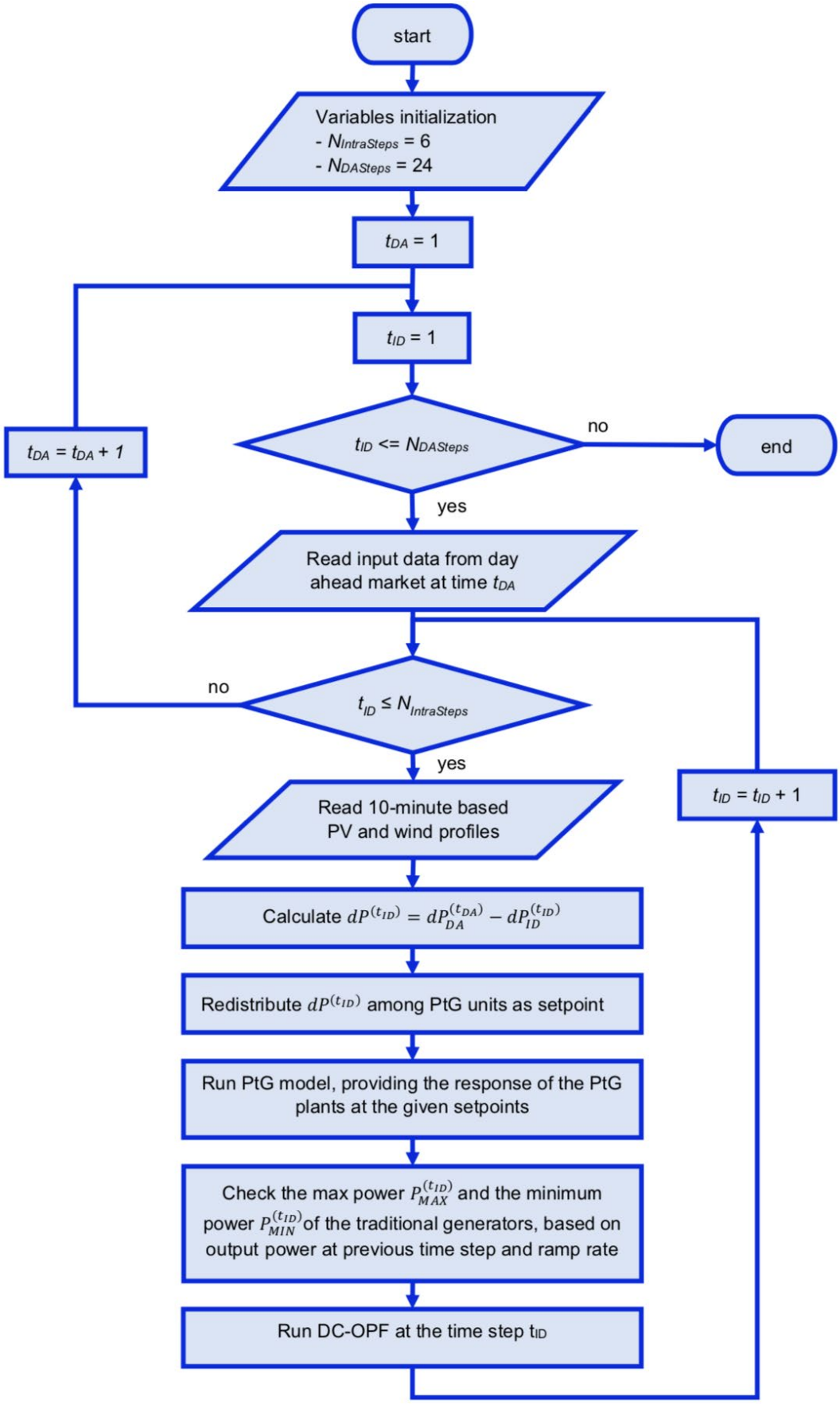

Figure 4-3. RTM flow chart [20]

The improvements to the code have been made only to the DA script, since computational time of the algorithm in figure 4.2.2 is quite limited: a whole day is simulated in less than 60 seconds, as there is no particularly heavy burden in the calculations.

The above mentioned PtG model needs a proper explanation, especially since it will also be recalled in the adjusted RT script.

4.2.3 PtG unit as a node in the loop

The setpoint of the PtG unit is calculated at the current time step of the RT algorithm, as a first order system response, thus needing only a determined number of past working points to quickly generate the current response. The N_{keep_step} helps the script execution by limiting the number of working points of the electrolyser, preventing the recalculation of past working points and simultaneously granting the model's accuracy with respect to the response obtained with the entire set of the points.

The model has been described with a function, taking all the PtG unit features as input: maximum and minimum power consumption and both current and previous states characteristics. In particular, H_2 tank level and N_{keep_step} history and current value are required for the model execution. N_{keep_step} should be equal or bigger than the selected time step in the ID script.

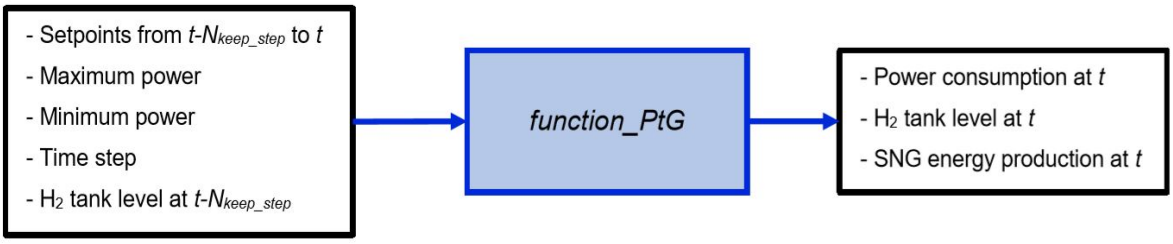

Figure 4-4. PtG model function [20].

Because of the PtG model higher resolution than RTM time steps, the model runs a number of one-minute iterations equal to the number of ID market time steps multiplied by the time step value itself. If the current time step is smaller than N_{keep_step}, all the past setpoints values are given to the PtG function as input, conversely, only the previous N_{keep_step} points are considered among the function inputs. Even so, the H_2 tank level needs to be as accurate as it can be, containing all the previous values. At each execution, H_2 tank level and the PtG absorbed by the PtG system are saved; at the same time, for each power to gas unit the average power represents the response of the unit itself at the current iteration, in the selected time step of the RTM.

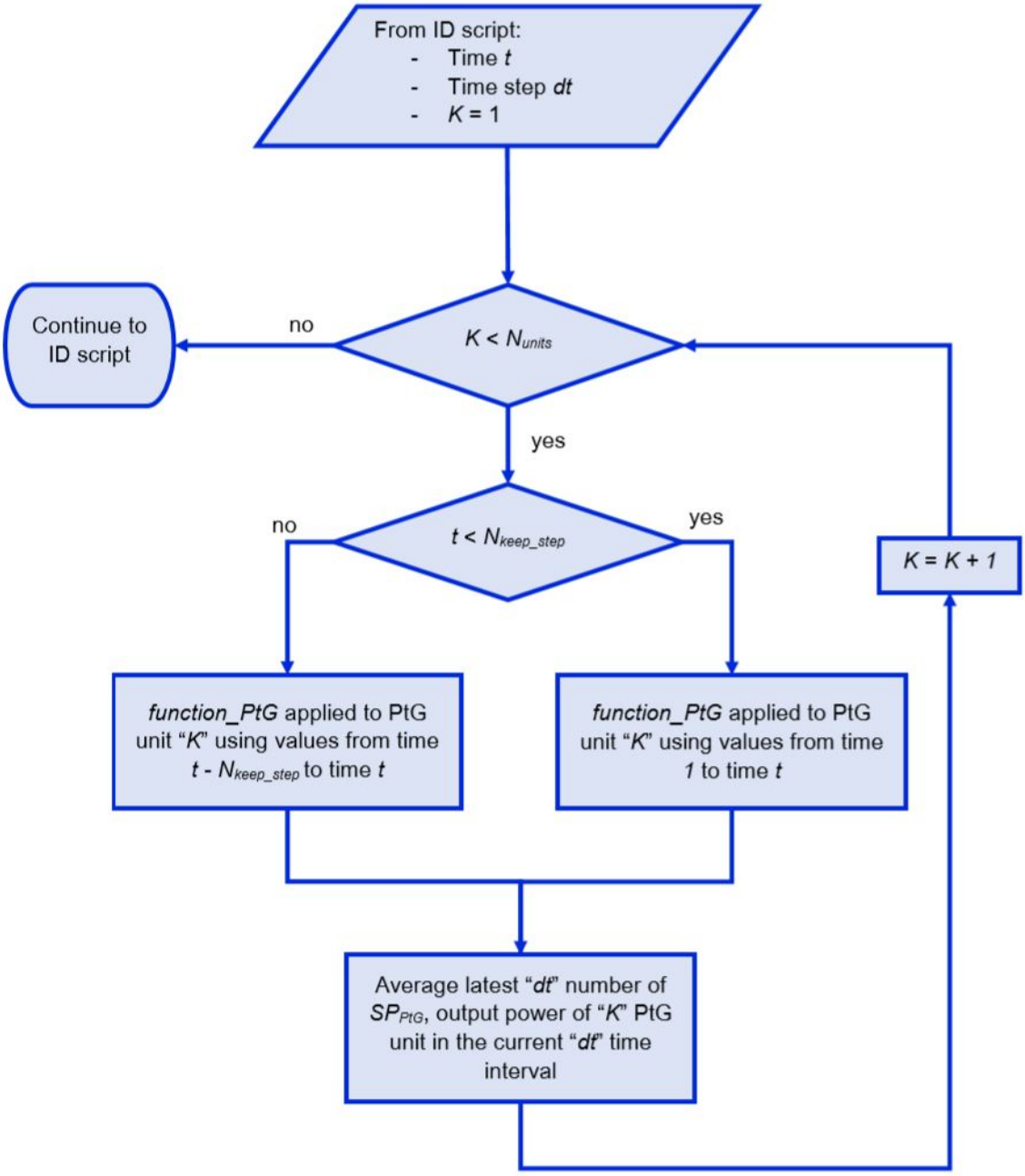

Figure 4-5. PtG flow chart representing PtG execution inside the RTM algorithm. [20]

4.3 MATPOWER

The description of the basic struct follows below.

4.3.1 *mpc* – MATPOWER Case

With reference to section 4.2, the MATPOWER case file contains all the essential details of the network configuration. All those pieces of information are contained in the subsequent fields of the structure:

- *mpc.bus*: specifically containing the values of the demanded power per node and in addition also loads position into the grid and the reference voltage value;

- *mpc.gen*: in which the maximum and minimum power output of the traditional generators are indicated for those units to be online, along with their ramp rates and their position in the network. Specific indexes have been created to address the different types of generators and easily manage them;

- *mpc.branch*: this field contains the information regarding AC lines parameters: extremes, resistance, reactance in pu, obtained as follows:

$$\frac{r_{380kV} * length_{km}}{Impedance}, \tag{4.1}$$

  the same is for reactance, whose values have been derived from Table 4.1. In addition, there are information on the lines' initial status and minimum and maximum angle difference;

- *mpc.dcline*: information on DC lines have been stored separately, as they are modelled as "dummy" generators, one with negative capacity, extracting real power from the network at the "from" extreme of the line, while the other with positive capacity injecting power into the network at the "to" extreme of the line. The real power flow p_f on the DC line at the "from" end is defined to be equal to the negative of the injection of corresponding dummy generator. Analogously, the real power flow p_t is equal to the positive injection of the related generator. Since the DCOPF does not account for losses,

$$|p_f| = p_t \tag{4.2}$$

  Thanks to this, DC lines can be assumed to be bi-directional. A graphical representation is provided in figure 4-6.

- *mpc.gencost*: gathers the data regarding the operation costs of generators, such as startup, shutdown costs. The model allows to express the cost function both piecewise linear and polynomial. The last two columns of the field indicate the: number of data points $(N+1)$ defining an n-segment piecewise linear cost function, or of coefficients defining a n-th order polynomial function and the parameters defining the total $f(p)$, where f is expressed in \$/hr and p in MW. Model = 1 corresponds to defining the cost by couple of coordinates $(f_1, p_1), (f_2, p_2) \ldots (f_N, p_N)$ where $p_1 < p_2 < \cdots < p_N$.

  Model = 2 corresponds to defining the coefficients of the polynomial function, starting with highest order, where cost is $f(p) = c_n * p^n + \cdots + c_1 * p + c_0$.

Table 4-1: Standard line types for overhead AC lines

Volt. Level (kV)	Wires	Series resist. (Ω/km)	Series ind. Reactance (Ω/km)	Shunt capacit. (nF/km)
220	2	0.06	0.301	12.5
300	3	0.04	0.265	13.2
380	4	0.03	0.246	13.8

*Data reported from [13].

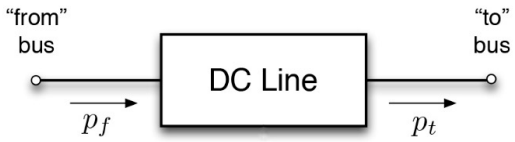

Figure 4-6. Equivalent DC line scheme

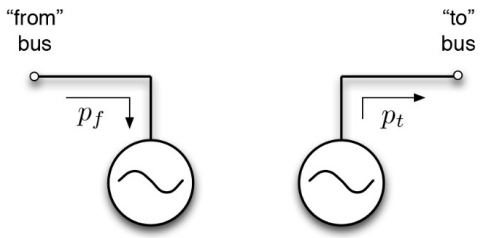

Figure 4-7. Equivalent representation of the DC line as two "dummy" generators.

The addition of the investments, as reported in Ch. 3.1, has been carried out in the *mpc* as well, in order to build the 2025, 2030 and 2040 scenarios. New lines have been added in the mpc.branch field, with respect to the following hypotheses assumed:

- lines belonging to the same zones have been clustered, in accordance with what has been done in [13];
- inter-zonal power transfer has been assumed bidirectional, thanks to the hypothesis of analysis without losses;
- for each investment, it has been assumed a corresponding line with the power transfer capacity equal to the maximum power increase indicated in [24], bidirectionally;
- whether an investment concerns an existing line, then its capacity is increased by the corresponding amount of power;
- only costs related to the single lines have been reported, in order to neglect intra-cluster connections;
- the indicated power transfers are related only to the corresponding areas and do not affect other zones' transfers, for what concerns the preliminary work.
- investments without information on either power transfer capacity of the lines or geographical location have been neglected.
- Capital cost is expressed in 10k€/km.

All the data relating to lines used for the model have been validated according to the parameters indicated in the Report of the Agency for the Cooperation of Energy Regulators (ACER) on “Unit Investment Cost Indicator and Corresponding Reference values for Electricity and Gas Infrastructure”.

4.3.2 Modelling and Problem Formulation

Matpower adopts all the standard steady state models typically used in power flow analyses, but as already introduced in section 2.1, only DC power flow is performed in this study, hence DC modelling alone will be presented.

The DC formulation is based on the hypotheses 2.1 to 2.4 and affects the data format. The matrices of the above described fields are composed of rows, to which single buses, branches or generators correspond and columns, indicating the information required in the fields.

The number of rows in *bus*, *branch* and *gen* are n_b, n_l and n_g respectively, while *gencost* has n_g generators, exactly as the *gen* field, since reactive power is not considered, thus also reactive costs.

Generators are modelled as real power injections at a specific bus. For generator i, the injection is p_g^i. $\mathbf{p_g}$ is the $n_g * 1$ vector of these generator injections, while the $n_b * 1$ vector of all bus injections from generators is expressed as

$$\mathbf{p_{g,bus}} = \mathbf{C_g p_g} \tag{4.3}$$

where $\mathbf{C_g}$ is a sparse $n_b * n_g$ generator connection matrix, whose $(i,j)^{th}$ element is 1 if generator j is located at bus i and 0 otherwise. The MW equivalents are specified in the column PG of *mpc.gen,* at the row i.

Constant power loads are modelled as a specified quantity of real power required at a bus: for bus i, the load is p_d^i.

$\mathbf{p_d}$ is the $n_b * 1$ vector of loads at all buses. Dispatchable loads are modelled as negative generators and appear as negative values in P_d, with associated negative costs. The negative power output assigned to the generator ranges from a minimum injection equal to the negative of the largest possible load to a maximum injection of zero.

To formulate the DC nodal power balance equations, it is sufficient to recall equations 2.11 and 2.13 and rewrite them within Matpower notation. The admittance matrix $\mathbf{B_{bus}}$ is obtained as the AC $\mathbf{Y_{bus}}$, the elements of the matrix have the same magnitude, with opposite sign: $\boldsymbol{B_f}$ (of the “from” end of branch) is equal to $\boldsymbol{B_t}$ (of the “to” end of the branch), hence

$$\boldsymbol{B_f} = [\boldsymbol{B}_{ff}](\mathbf{C_f} - \mathbf{C_t}) \tag{4.4}$$

$$\mathbf{B_{bus}} = (\mathbf{C_f} - \mathbf{C_t})^{\mathbf{T}} \boldsymbol{B}_f \tag{4.5}$$

where $\mathbf{C_f}$ and $\mathbf{C_t}$ are the $n_l * n_b$ sparse connection matrices built considering the $(i,j)^{th}$ element of $\mathbf{C_f}$ and the $(i,k)^{th}$ of $\mathbf{C_t}$ as 1 for each branch *i*, if it links the bus *j* to the bus *k*, and zero for all the other elements.

Thus, by neglecting shunt elements, that are not connected to the network in object, the DC equations follow in the same form of the 2.11:

$$\mathbf{g_P}(\boldsymbol{\delta}, \mathbf{p_g}) = \mathbf{B}_{\text{bus}}\,\boldsymbol{\delta} + \mathbf{p_d} - \mathbf{C_g}\mathbf{p_g} = 0 \tag{4.6}$$

The costs assigned to the generators of the network have been expressed through the coefficients of a 1st order polynomial function, according to “Model 2” of the *mpc.gencost* column.

PtG units, modelled as dispatchable loads, have been assigned a high cost in order to ensure their dispatch, while RES generators have been set to a zero cost, since they are intended to be dispatched with higher priority with respect to traditional generators.

4.4 Genetic Algorithm

In optimization theory, often used in operations research, a genetic algorithm is a metaheuristic process belonging to the larger class of evolutionary algorithms, inspired to Darwin's theory of evolution, that relies on the bio-operators of crossover, mutation and selection to produce an optimal population leading towards better solutions for the optimization problem to which it is applied.

This type of algorithms, developed by J.Holland in the 1960', improved and extendend by Goldberg more than 20 years later [36], is widely used in optimization problems because of their simplicity of implementation and for the quality of the solutions provided. In fact, although not being able to converge to the global optimum, but only to the local one, the quality of the solution is customizable by the user in both the definition of the fitness function and of the termination criterion.

4.4.1 GA features: selection, crossover and mutation.

The algorithm is based on a population of candidate solutions. Each of them has a set of properties, i.e. its chromosomes or genotype, that are subjected to alteration by genetic operators: crossover and mutation. Traditionally, the chromosomes are represented as strings of binaries 0 and 1. In the standard version, the "evolution" starts with a population randomly generated, whose chromosomes are selected for reproduction: first the recombination or crossover occurs, where chromosomes form a new string, the offspring, then a mutation may occur, altering the elements of the string. The random construction process of the initial population allows the entire range of search space to be explored by the algorithm. The subsequent selection process takes place through the fitness function. The fitness of an organism can be measured by its success in staying alive and usually represents the objective function of the problem being solved, as well as the quality of the corresponding solution, as in expression (4.7). The "fittest" individuals are stochastically selected from the current population and each individual's genome is modified, according to the probabilities set for genetic operations to occur. Crossover is realized by a cut and paste of a part of a selected string into another, as in fig. 4.4.2, so that the final size of the modified chromosome is equal to the initial's: chromosomes size may also vary, as the crossover point may be single or multiple, but the process complexity rises accordingly. Conversely, mutation is the genetic operator responsible of population's genetic diversity, it consists of the alteration of genes values contained within the selected string, from 1 to 0 and vice versa, as represented in fig. 4.4.2 below. The probability of alteration is user definable and should be set low, as high values would turn the operator into a primitive random search. The position of the mutation within the chromosome may be predetermined or randomly decided at each iteration as well.

During the process of evolution of the population, the best organism of the current generation is carried over the next, unaltered: this strategy follows the elitism principle, which allows the GA solution not to worsen over the successive generations. The generational process repeats itself until the termination criterion is satisfied. Possible conditions are:

- The minimum criteria are met by a solution;
- The fixed maximum number of iterations is reached;
- A number of iterations without significant improvements has been reached.

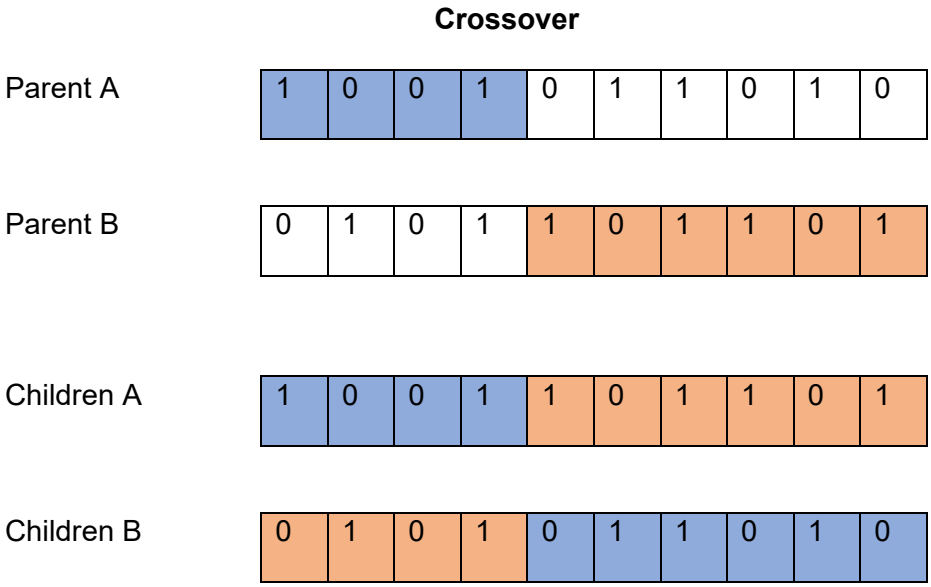

Figure 4-8. Representation of Crossover operator

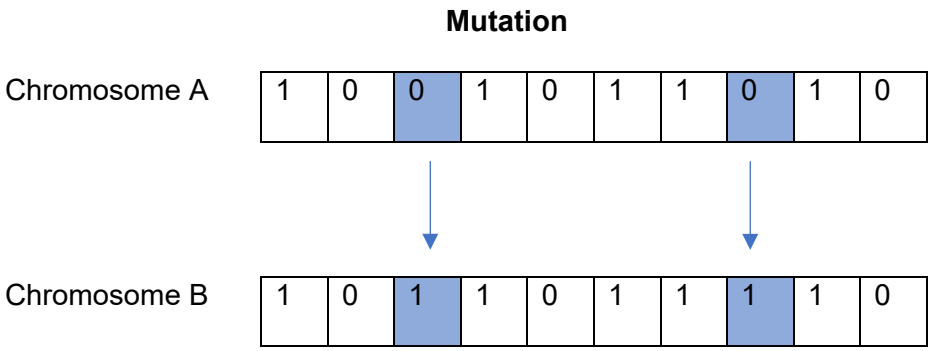

Figure 4-9. Representation of Mutation operator

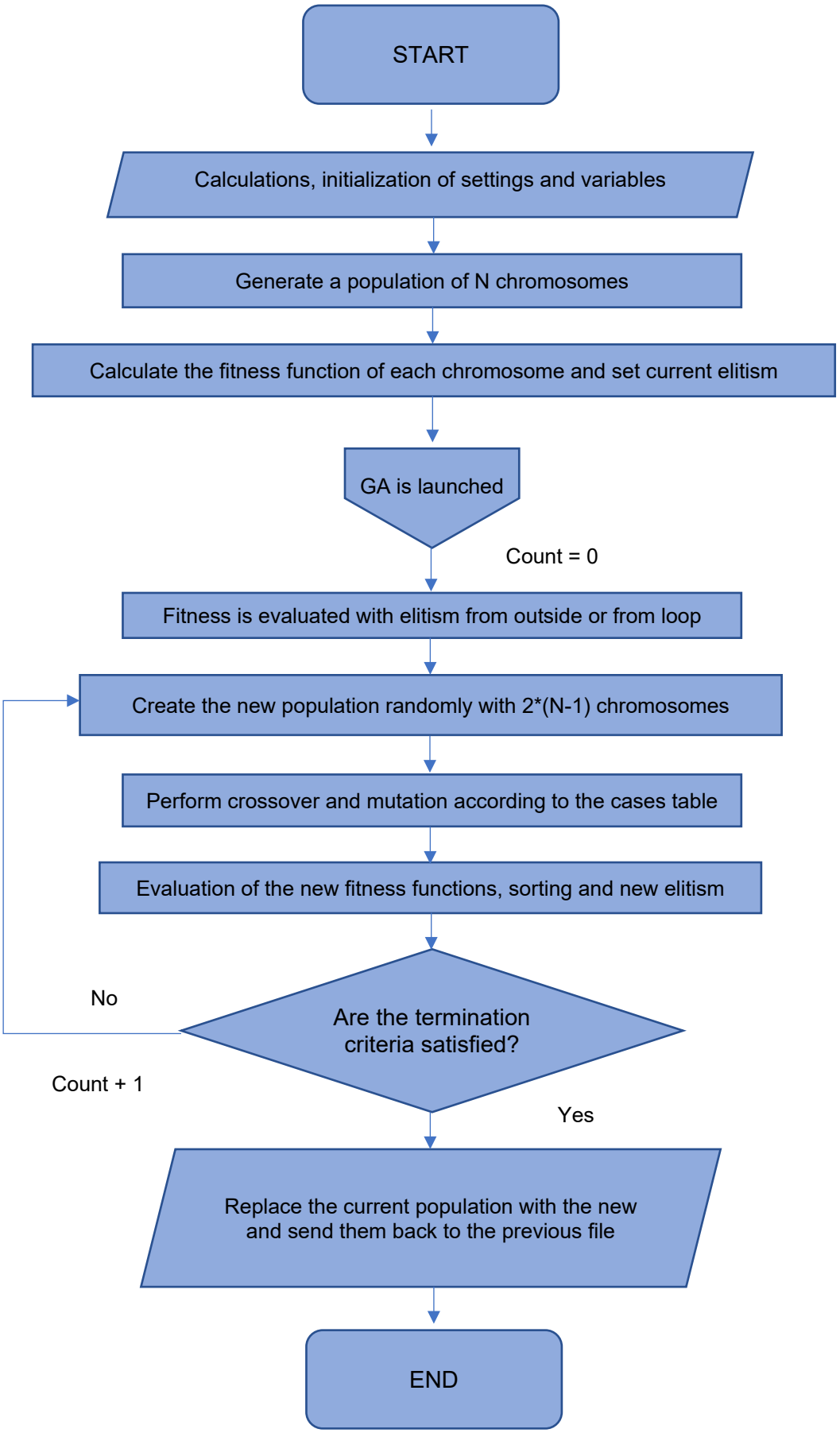

Figure 4-10. GA flow chart

The Genetic Algorithm has been developed within the code structure, adapting it to the Matpower framework, to accelerate the Unit De-commitment process, that previously relied on a deterministic algorithm. As a matter of fact, the *runuopf.m* file has been modified, along with *uopf.m* file: at the beginning the original *mpc* file is saved, then the algorithm parameters are set (such as the number of chromosomes, the probabilities of crossover and mutation and the percentage of generators that become candidates to by shut down by the algorithm).

The selection of the candidates is based on a filter applied to the generators violating the minimum power constraint: a function is created by multiplying the minimum power constraints values by generators' minimum power, which is used as weight. The generators to be submitted for the optimization process are represented by the highest values of the abovementioned function, sorted in descending order. The final number of candidates is taken by rounding to the nearest integer number the product between the selected percentage and the total number of initial candidates activating the above constraints.

The first population of strings, that represents candidates status (0 for 'offline generator', 1 for 'online generator'), is created through a matrix of random numbers between 0 and 1, with size equal to the number of chromosomes as rows and the number of candidates as columns. Another matrix, made of ones, is created with the same dimensions. The indices of all the elements of the first matrix smaller than 0.5 are linked to the elements of the latter matrix, that are consequently put to zero and hence providing the first list of generators to shutdown to minimize the total cost for serving loads.

The successive step is the calculation of the objective functions of the optimization problem. The evaluation is carried out in parallel computing to save time, since it requires a number of DCOPF equal to number of chromosomes to be performed at once. The **selection** stage starts with the fitness functions computation, performed by inverting the objective functions: the maximum is taken, as well as its index, to be both passed to the actual Genetic Algorithm function as the best configuration found and inserted into the population as result.

The GA receives as input the initial population, the fitness values, along with the first elitist configuration, the setting parameters and the remaining required variables (*mpc*, *mpopt*…). The loop is started by initializing a counter variable, keeping track of the number of iterations performed. The Cumulative Distribution Function (CDF) is calculated at this step by means of a cumulative sum of the fitness function values and then normalized to the sum of all the fitness values, so that the sum of all resulting fitness values equals 1, as below.

$$\psi_i = \frac{\frac{1}{(f_{b_i})}}{\sum_{j=1}^{N} \frac{1}{(f_{b_j})}} \tag{4.7}$$

where *N* is the number of chromosomes and thus of fitness functions f_{b_i}, hence

$$\sum_{i=1}^{N} \psi_i = 1 \tag{4.8}$$

The accumulated normalized fitness values can be described as follows:

- the accumulated fitness value of a chromosome is the sum of its own fitness value plus the fitness values of all the previous individuals
- a random number is extracted from a uniform distribution in the interval [0,1];
- each random number is used to enter the vertical axis of the diagram, obtaining the corresponding number of string from the horizontal axis;
- the same string may be selected more times;
- the selection stage is based on the ***biased roulette wheel***, that is the strings with higher normalised fitness have a greater probability to be chosen, though all strings having a certain probability to be selected.

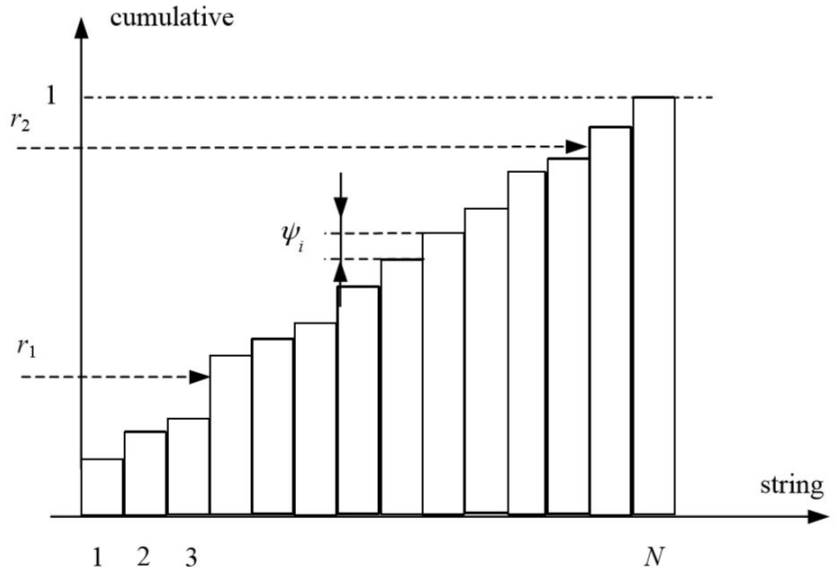

Figure 4-11. Strings selection through random extraction [37]**.**

This process has been executed in the Matlab script within a larger loop that comprehends the genetic operations as well, repeating itself for 2*(N_c-1) iterations, i.e. the number of elements composing the new population. Probabilities are determined with 3 extractions: the first for population creation, the second and third for Crossover and Mutation, respectively. The values of the first random extraction are compared with the CDF values, picking the ones smaller. If the smallest value is picked, 0 would be consequently returned as index, then the index is set to 1, indicating the first-string selection; otherwise, the maximum index is taken and used in the population construction. The number of elements of the population has been widened because of the crossover operation: in order to cut a part of the string both from parent A and B and paste it into the offspring chromosomes, in swapped order, the operation can only take place between a couple, as in fig. 4-8. Thus, the number of original chromosomes, minus the elitist one, is doubled. For the same reason, this operation can occur only when the index of the loop that cycles chromosomes is even. On the contrary, mutation can take place at each iteration, thus creating two scenarios with different cases, as described below in the cases table.

Legend

extrC = extraction for crossover, *pCross* = probability of crossover

extrM = extraction for mutation, *pMut* = probability of mutation

- if *extrC* > *pCross,* 1 is assigned to the event that occurs, otherwise 0 and the event does not occur;
- If *extrM* > *pMut,* 1 is assigned to the event that occurs, otherwise 0 and the event does not occur.

If the index is even:

Table 4-2a

CASE	CROSSOVER	MUTATION
1	0	0
2	1	0
3	0	1
4	1	1

Otherwise:

Table 4-2b

CASE	CROSSOVER	MUTATION
1	0	0
3	0	1

In the crossover operation the cutting point is single and randomly determined, while for mutation the number of alterable genes has been previously set to 5, while the actual positions of mutation are determined randomly as well during the loop, at each iteration. According to the table, when both operators act, first crossover is executed, then mutation operates over the same chromosomes.

Once created the new population, the corresponding objective functions are evaluated, sorted in descending order and the new fitness functions computed. The maximum fitness value is taken and compared to previous elitist one: if the objective function improves, the corresponding string is added to the population and the elitist configuration updated, otherwise the elitism is preserved, and the stop criteria are checked.

If $$\left|\frac{f_{bi}^{1} - f_{bi}^{0}}{f_{bi}^{0}}\right| < \varepsilon \quad (4\text{-}9)$$

an auxiliary counter is increased up to 5 (one count per round), otherwise it is put to zero, so that the algorithm may keep iterating even though (4-9) is immediately satisfied. On the other hand, the main counter is increased at each iteration. If the auxiliary counter is equal to 5 or the main counter reaches 10 the loop ends. $\mathcal{E}$ is set to *1e-6*, the number of iterations should be higher in order to obtain a good quality of the solutions, but since GA converges quickly to acceptable optimal solutions, a trade-off between the quality of the solution and speed has been made.

When termination criteria are not satisfied, fitness, objective function, population values are updated and counter is increased, hence a new iteration starts.

The main advantage provided by the GA implementation to the code is definitely the speed: it allows to run a monthly simulation in barely 2 hours.

4.5 DAM adaptation

As a result of the advantage provided by the GA, in terms of computational time reduction, the DAM script has been modified in order to allow the simulation of multiple days, instead of one.

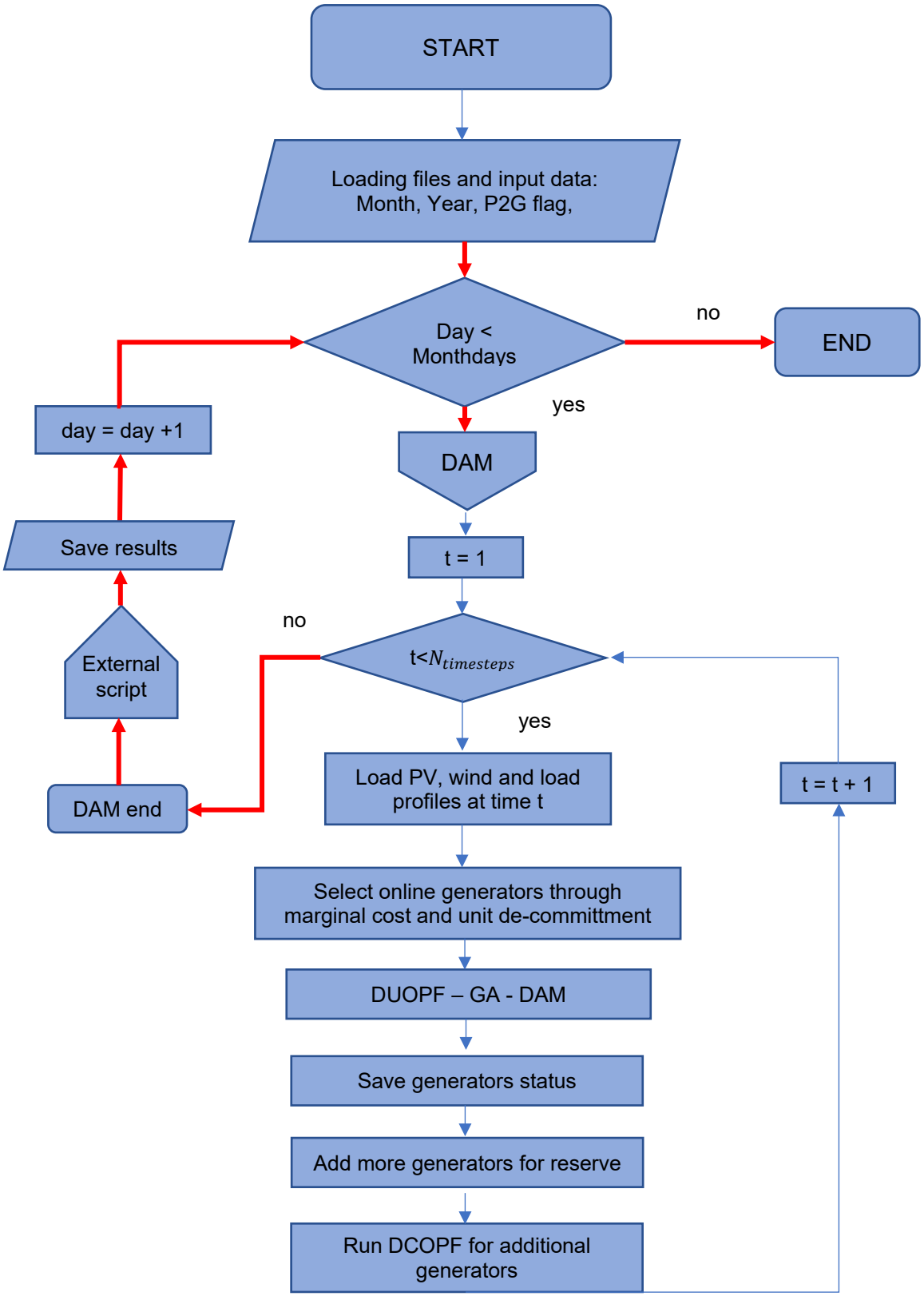

Figure 4-12. Modified DAM flow chart

With respect to the previous flow chart, the day ahead market script has been converted into a function, that is called into a new script, called “DAM_month”, in which the monthly loop is created, as well as the instructions to pass the inputs to the DAM function and to save its daily results. In particular, the most relevant data to set as preliminary step are: month, year and type of year (dry, wet…) selected and *mpc* (representing the grid scenario) as objective of analysis and the power-to-gas flag, that allows to enable or disable the PtG units properly installed into the grid. With such modifications, highlighted in red, it is possible to decide whether to simulate a whole month, a single day or a week.

4.6 RTM adaptation

The same modifications have been applied to the IDM script, in order to simulate up to a month.

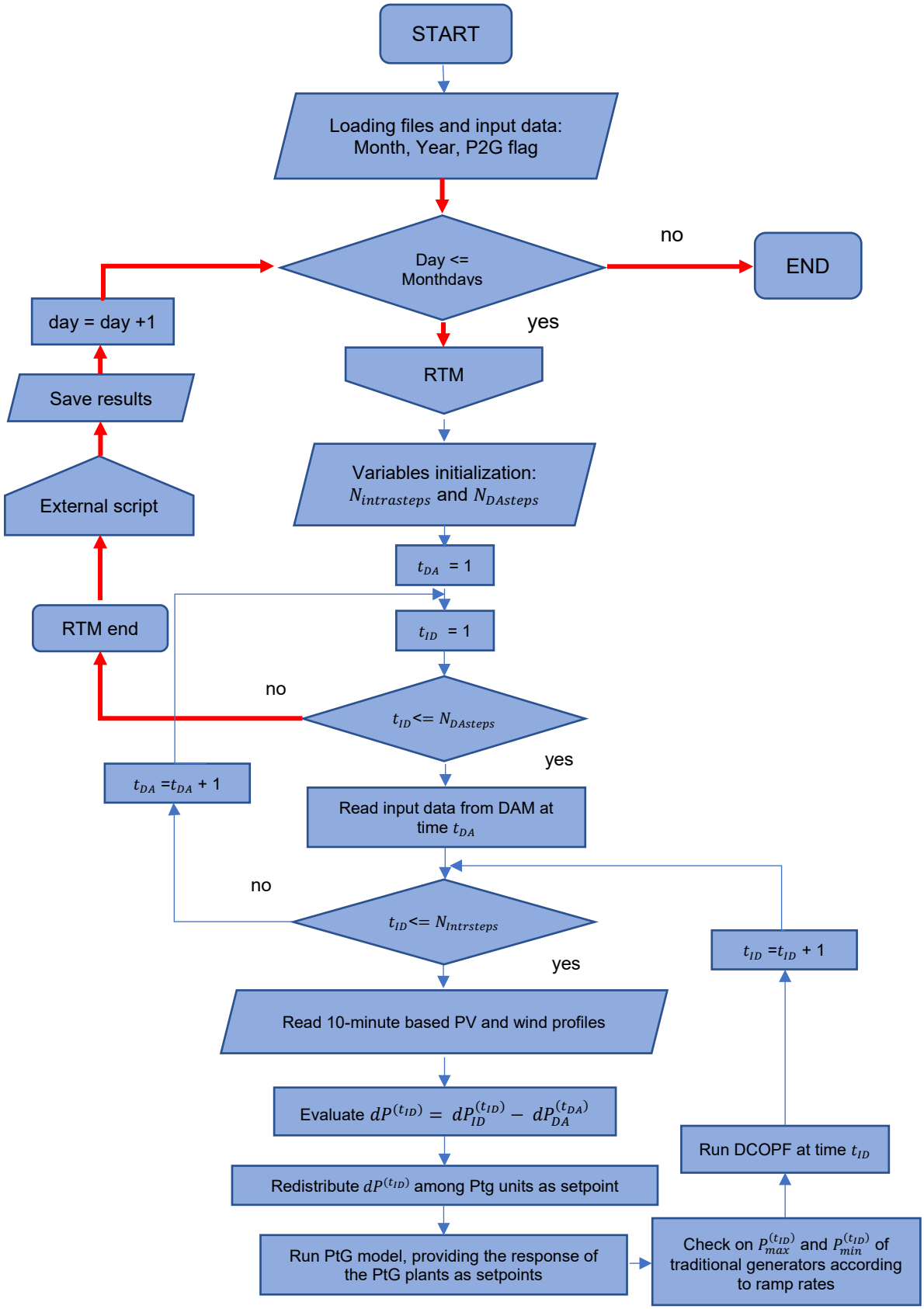

Figure 4-13. Modified RTM flow chart

The ID script has been converted to function as well, in order to be called within the monthly loop at each iteration. The input data are once again month, year and type of year, the PtG flag option and the *mpc,* that allows to select the grid scenario. After each iteration, daily results are saved to be analysed later. With respect to the previous version, the variation of renewable power produced $dP^{(t_{ID})}$ from the average value has been evaluated between the intra-day value and the renewable DA dispatched output, instead of renewable DAM profiles: that is because of the fact that RES are now constrained to a minimum power output of 15% (average value) of the maximum, it happens that not all of them are actually or fully dispatched in the day-ahead market.

4.7 Scripts for analysis

The results of the simulations are usually divided by month (it depends on the length of the simulated period), thus it is convenient to analyse them by means of a loop that loads them in monthly steps.

In the first part of the code, before the loop starts, all the needed variables required for calculations are initialized. Most of the data existing in the structures saved into simulations 'results are in the matrix form, hence it is necessary to organize these data in other structures or 3D matrixes in order to create monthly archives of valuable information. Specifically, it is possible to select the month and the year of which simulated data will be analysed, the folder which they will be loaded from and other features that distinguish them, such as: the network scenario used to get them and the optional presence of PtG units.

To provide a few examples of data of interest, it is possible to start from the need of organizing all the data regarding the lines in two sets: lines that can be sorted by country of belonging and trans-national lines, with the aim of detecting the geographical location of events of concern, such as congestions. The objective of these analyses is to detect both lines congestions and also other information, that are sensitive for the PtG placement: nodal RES net power. To be more precise, PtG technology is most effective when combined with a renewable source, in areas that show abundance in terms of CO_2 availability, as explained in Ch. 3. Consequently, it is necessary to analyse in which buses there is a surplus of renewable generation, exceeding loads demand: these locations are suitable candidate for PtG units sites. The idea is to place PtG units in nodes presenting continuous and abundant occurrence of renewable surplus and congested lines connected to them, with the target of absorbing generated power, thus reducing power flow on the problematic line.

4.7.1 Congestions

Since congestion alleviation through PtG technology is one of the main objectives of this thesis, it is appropriate to provide a definition. Power grid congestion is a situation wherein the existing transmission lines are unable to accommodate all required loads, during periods of high demand or during emergency load conditions, because their power capacity is saturated creating bottlenecks for electricity flows. This type of event may take place when an adjacent line is taken out of service or damaged or when power flows exceed lines capacity. Congestions affect both grid's reliability and efficiency, leading to a significant or even exponential increase of line losses under high load conditions, this occurs also when lines operate near their thermal limits. Although efficiency and losses not being tackled by this study, the congestion of the lines has other implications worthy of interest and inherent to this research direction: during periods of high demand, electric retailers may not have access to

the cheapest source of electricity, because the market splits and in order to guarantee power delivery more expensive generators are dispatched, to cover up higher need for electricity. This aspect directly implies that consumer prices can be driven to very high levels in such conditions, hence translating into an increase in the total system costs, in other words the global economic efficiency of the power system decreases. As a matter of fact, although the system is able to continue to operate reliably, it does come at an additional cost: both expensive generators and reserves go online, as result companies operating them must be compensated accordingly. To provide a real example of the total cost of congestion, it is possible to give the German case, in which the cost of redispatch weighs on consumers by more than 1.4 billion euros per year [38].

5 Results of the simulations based on ENTSO-E GCA scenario

5.1 Global Climate Action Scenario

The analysis of the clustered network operation has been carried out under the 2040 GCA scenario [30], that is the most restrictive from the perspective of decarbonisation and penetration of renewable sources' objectives to be achieved. As a matter of fact, in this scenario global methods towards CO_2 reductions are implemented. First of all, the presence of an efficient ETS trading scheme is assumed, i.e. the European trading system for greenhouse gas emission allowance, because of its key role in providing to the electricity sector the means to successfully contributing to the EU and global decarbonisation objective. In addition, a CO_2 market provides the price signals triggering investments in low carbon power generation technologies. A technology neutral framework is established to support investments in renewables: wind generation is expected to reach the 34% of the total demand, while solar generation the 17%. Power-to-Gas becomes a commercially viable technology for green gas production, according to the methodology presented in ANNEX II of the report [31], by ENTSOG. CO_2 price makes natural gas-fired CCGTs cheaper than coal, being suitable for providing flexibility to the electricity market. On the contrary, nuclear depends heavily on countries specific policies, but still there may be potential for a limited number of new units in some countries. Carbon capture and storage will be fostered for those industries, whose processes are characterized by high load factors, though still not being economically viable. System adequacy is driven by price signals, allowing a solid increase of market-based investments for the construction of new power plants. The implementation of global climate schemes improves the competitiveness of energy intensive industries within Europe. Yearly electricity demand is expected to grow considerably by 2040 because of increasing electrification of final uses in various sectors, although this being limited by energy efficiency improvements. The measures to address heating systems' enhancement consist in fostering the installation of electric and hybrid heat pumps in high efficiency and low efficiency buildings respectively. Transportation sector is heavily affected by GCA actions as well: the transition towards electric vehicles is strongly encouraged and towards LNG for the segment where electricity does not represent an alternative to gasoline, i.e. shipping sector and heavy goods. As a matter of fact, it is forecast that gas demand will increase in the transportation sector, it will decrease in the residential one and will remain stable for industrial sector. Finally, consumer behaviour is expected to be influenced by demand and response, made possible by increased automation in residential technology and Internet of Things, it will encourage users to shift their demand of power to low-priced hours. Demand and response represents a key factor to ensure system adequacy, thanks to the shift of demand peaks.

GCA scenario is implemented into the code by means of generation and load profiles datasets, that are available in three variants, representing three different climatic conditions:

- **1982** for dry weather conditions;
- **1984** for normal conditions;
- **2007** for wet weather conditions:

Further information on the features of this scenario can be found in [30].

5.2 Simulations settings

From the computational times obtained in the daily simulations of the network, with the scripts described in the Section 4, it has been decided to represent the performance of the network in the reference year of the selected scenario by simulating the operation of the network in four months. The four periods chosen, one per season, are: January, April, July and October to adequately take into account the variations in load and generation due to seasonality during the year.

The selected grid configuration for the simulations reflects the aims of the study: to highlight the positive effect of PtG technology within the network. Appropriate conditions have been chosen in order to reach the goal:

- Grid configuration is the 2025 version;
- Load and generation scenario is 2040 GCA;
- Normal climatic conditions, i.e. “Type of year: 1984”.

First of all, the investments planned for the 2025 horizon are considered to have been completed, since network planning for this horizon is already accurate: the additional infrastructure, i.e. lines, transformers, etc., is already in construction. Besides, the GCA context has the highest percentage of load and generation increase, due to an accelerated electrification of end uses. This grid configuration allows to evaluate the worst operation scenario: the network is subject to higher load with respect to present and has to endure a higher percentage of perturbances.

In order to correctly place the PtG units, day-ahead and intra-day simulations have been performed throughout 2040.

5.2.1 PtG units placement

Before describing the placement procedure, introduced in section 4.7, it is convenient to recall PtG requirements. PtG units must be fed by renewable sources to absorb excess production. Besides, it is also ideal to install this type of plant in places with an abundance of CO_2. Finally, to increase the effect of congestions relief, it has been decided to adequately install, where possible, units of appropriate size in the proximity of the congested lines.

Therefore, it is possible to summarize the positioning procedure into a sequence of steps, following three criteria that candidate nodes need to meet:

- Considerable amount of non-dispatched renewable energy;
- Connection to congested lines;
- Presence of CO_2.

From DA and RT simulations results, monthly data have been aggregated to obtain a yearly perspective, thus it has been decided to base the procedure on the data obtained from the real time analysis, because of the higher resolution of the model.

The first step consists in detecting the congested lines over the month, afterwards the nodes connected to those lines are gathered. Once collected the information for the four months

simulated, the number of occurrences of the nodes over the year is counted, hence the list of nodes related to congested lines is created and ranked in descending order.

Similarly, it is computed the amount of available RES power per bus, along with the dispatched power per bus, thus a subtraction allows to derive the amount of RES power at possible disposal of PtG units. Such a list is created by ranking these values and then repeating the procedure for the other months: the most recurrent nodes showing this renewable surplus are selected as privileged candidates.

Finally, these two sets are intersected to a third, which contains the amount of power that can be installed thanks to CO_2 availability in each of the grid nodes. Candidates belonging to the resulting list are the selected for the final placement.

The total amount of power-to-gas to be installed in the simulated grid represents the last constraints of the procedure. To reach the 16.85 GW of PtG power computed in Section 3.2, it is not sufficient to consider only the most suitable candidates, on the contrary, the list must be enlarged by considering the highest-ranking nodes and the corresponding availability of CO_2 throughout the year by their occurrences.

At the end of this process 21 PtG plants have been placed within the following locations:

- In 2 buses in Austria;
- In 1 bus in Switzerland;
- In 6 buses in Germany;
- In 1 bus in Denmark;
- In 5 buses in Spain;
- In 1 bus in France;
- In 4 buses in Italy;
- In 1 bus in Netherlands.

The positions within the clusters can be observed in the following figure 5-1.

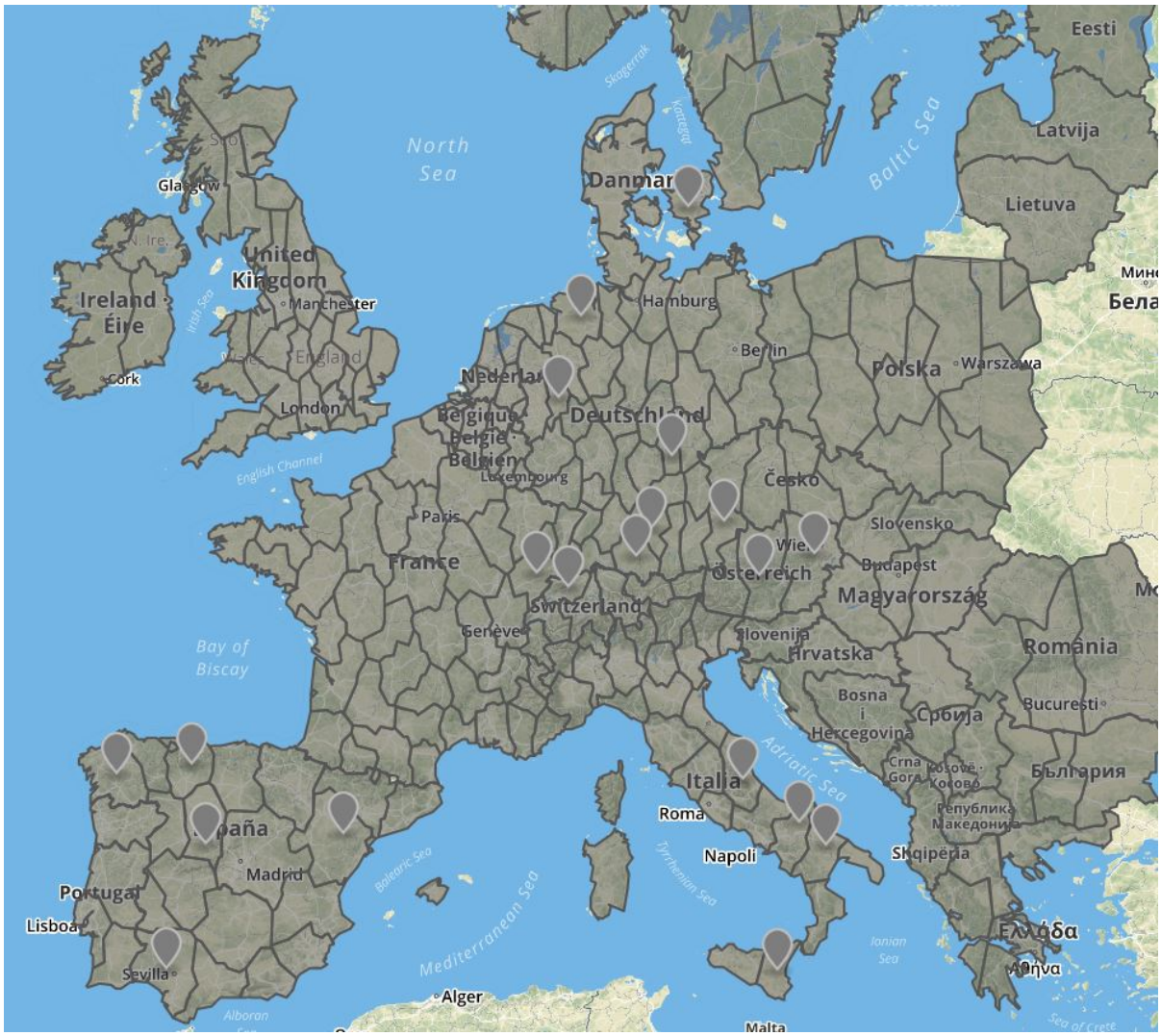

Figure 5-1. PtG placement. Visualized through www.geojson.io.

The results of the procedure finds confirmation on the status of the actual network for what concerns the validity of placement, since lots of the PtG nodes corresponds either to weak zones of the network as the Southern Italy area or the heavily loaded lines connecting Northern Germany to Southern Germany (objective of massive investments for grid enhancement, as indicated in [24]), or simply to areas having plenty of unexploited renewable potential, as Northern and Central Spain and Germany itself.

5.3 Simulations results

After the positioning of PtG units in the nodes indicated, DAM and RTM simulations have been run to evaluate their contribution to the network operation. The capacity of the lines has been set to the rated value, neglecting security parameters because of the level of accuracy adopted for lines characteristic parameters, while a minimum output power has been set for renewables (~15%, this value represents a compromise between real values and simulation needs), to reflect adequately the real conditions, both in DA and RT. Results indicate that network performances globally improve as illustrated in the following figures. Besides, it is also evident that PtG increases renewables dispatch.

5.3.1 DAM analysis

The first analysis has been performed to compare the DA operation of the 2025 grid, under the 2040 GCA generation and load outline, with and without the effect of the PtG units. To obtain yearly results, four simulations have been executed on the reference months, firstly with the original grid and afterwards with PtG technology enabled. In DA operation, PtG has been inserted by limiting absorbed power to 60% of the rated installed capacity, with the aim of preserving a wide margin of adjustment to be exploited for real time deviations to dispatched power.

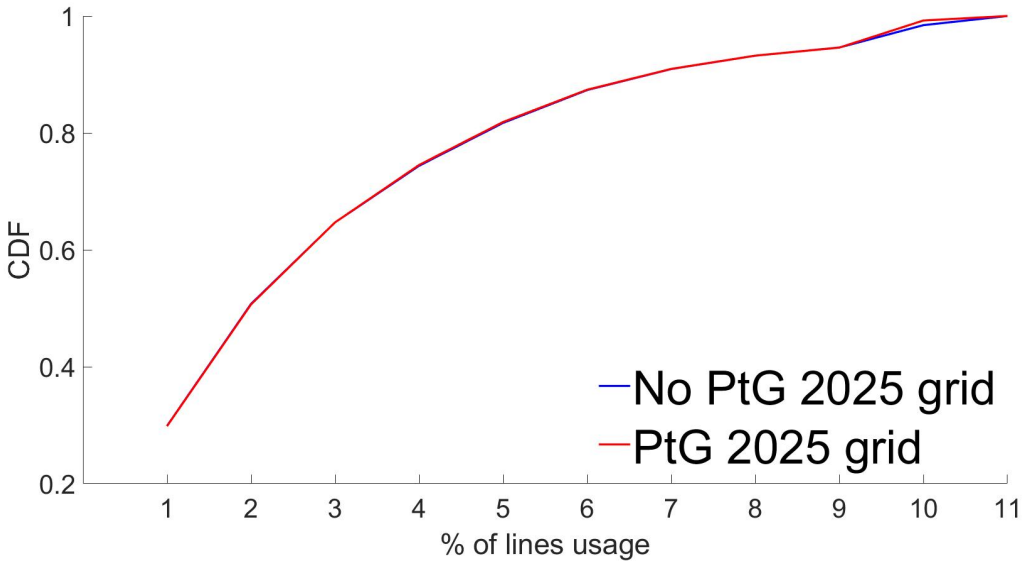

Figure 5-2. CDFs of congested lines for year 2040 in DAM simulation.

The figure 5-2 represents the cumulative distribution function of the congested lines throughout the four months of 2040 of the DA simulation. To build this curve, eleven classes have been created to rank all the 508 lines of the network according to the percentage of load to which they are subjected, with respect to their rated capacity. The last class represents the overloaded lines. To fill the classes, the values per time unit of the ratio between the power flow on the lines and their nominal capacity have been taken, recorded over the days of the month. The total number of elements n_{el} that have been inserted into the classes is $n_{el} = n_{lines} * n_t * n_{days}$, where n_{lines} is the total number of lines, 508 for 2025 grid, n_t is number of time units of the day, 24 hours in DA analysis and n_{days} is the number of days contained in the months analysed (123 if considering January, April, July and October).

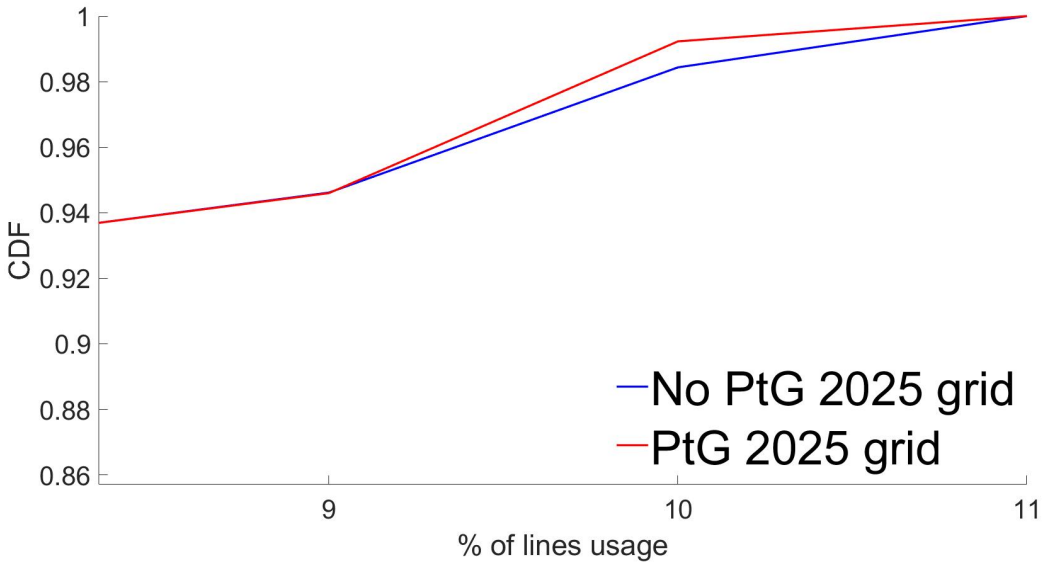

Figure 5-3. Detail of CDF curve for DA simulation of 2025 grid in 2040 scenario

To better understand the meaning of the CDF curve is convenient to zoom in the figure, as a matter of fact, it is possible to notice that PtG units have reduced of the 51% the number of elements belonging to the overloaded lines class and increased of the 21% the numerosity of the 100% class, meaning that the missing congested lines have returned to normal operation conditions, thus fully exploiting their rated capacity.

For what concerns RES dispatch increase, results have been analysed by aggregating the values of the hourly output dispatch of the market into monthly values and then yearly ones. It is interesting to notice that for DA simulations PtG helps increasing a little bit the characteristic and thus prevailing renewable source of the month considered: for example, in January wind is prevailing over solar and hydro sources.

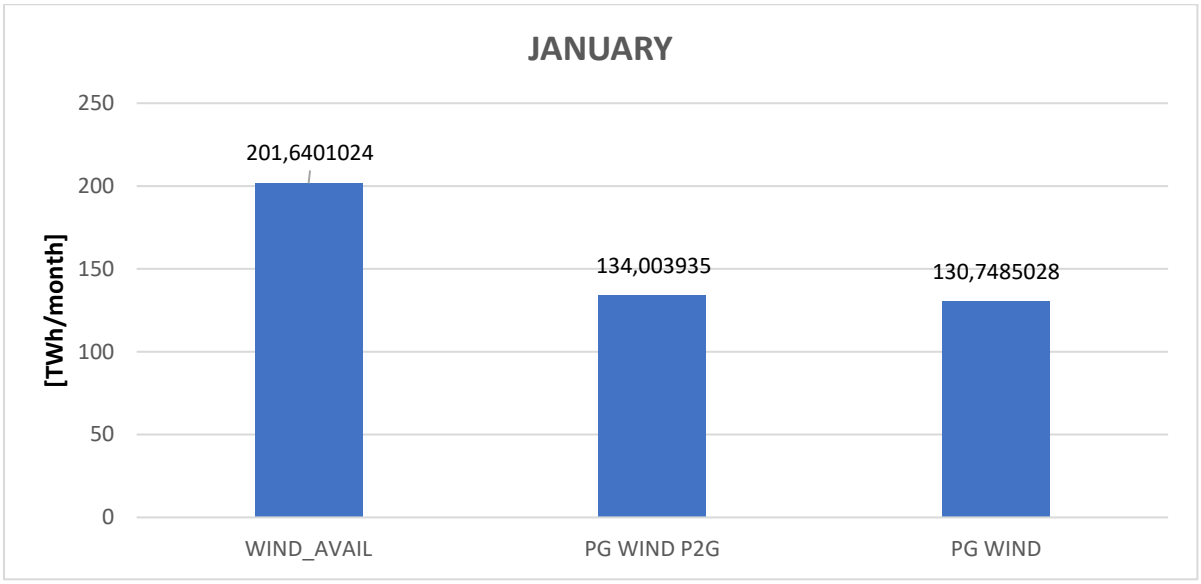

Figure 5-3. Comparison among Wind availability, Wind power produced with and without PtG in January with 2025 grid.

Thanks to PtG effect, wind production increases of the 2.5% in January. Analogously, in April PV and ROR increase of the 3% and 1.25%.

Figure 5-4. Comparison among PV availability, PV power produced with and without PtG in July with 2025 grid.

In July, when solar power plants are at their maximum power production, PtG effects produces an increase of 3.5% in production. Whereas in October it is again wind to score the highest percentage increase with a 4.9%, while ROR production grows of the 3.7%.

5.3.2 RTM

The second set of simulations has been performed on a similar configuration, but within the RTM context, with a time unit resolution of ten minutes. In this case the number of elements of the classes increases, since a higher temporal resolution leads to a greater number of time unit in a single day, as a matter of fact $n_t = 144$.

Besides the resolution, there is another difference from DA conditions, as a matter of fact PtG profile power for RT is not set to 60% anymore, but it is adjusted to the nominal power of the plants, to provide the maximum flexibility for regulation services.

Results on lines congestion data show a similar trend as the DA ones. In fact, congestions recorded in the overload class diminish by 49.5%, being redistributed to the lower classes and hence improving the utilisation of the available capacity: the 100% class presents an increase of 20%.

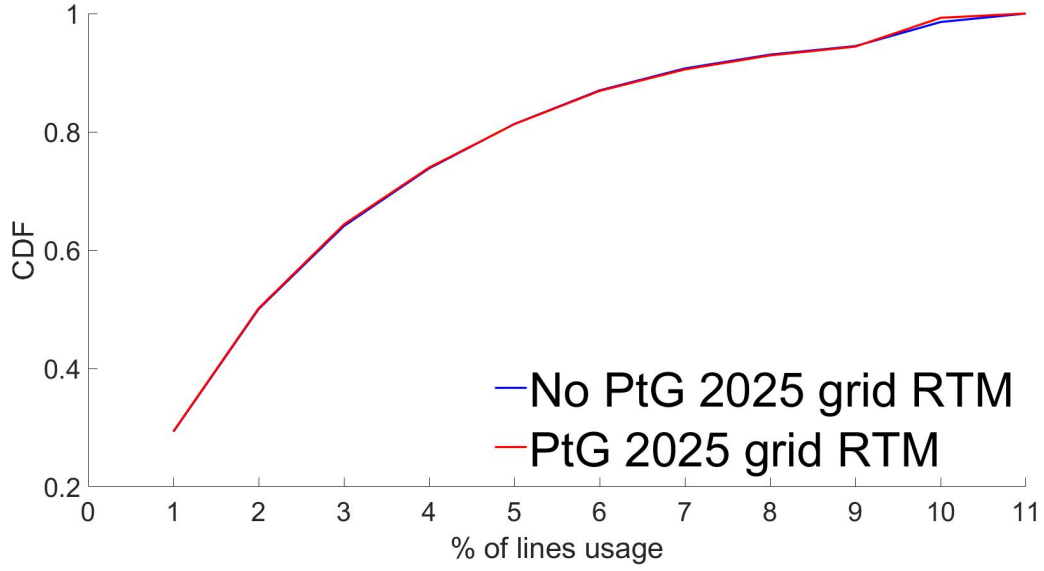

Figure 5-5. CDFs of congested lines for year 2040 in RTM simulation with 2025 grid.

A detail outlook on the CDF curve clarifies the variation in the upper classes, giving an insight also about the smaller variation of the lower ones' values.

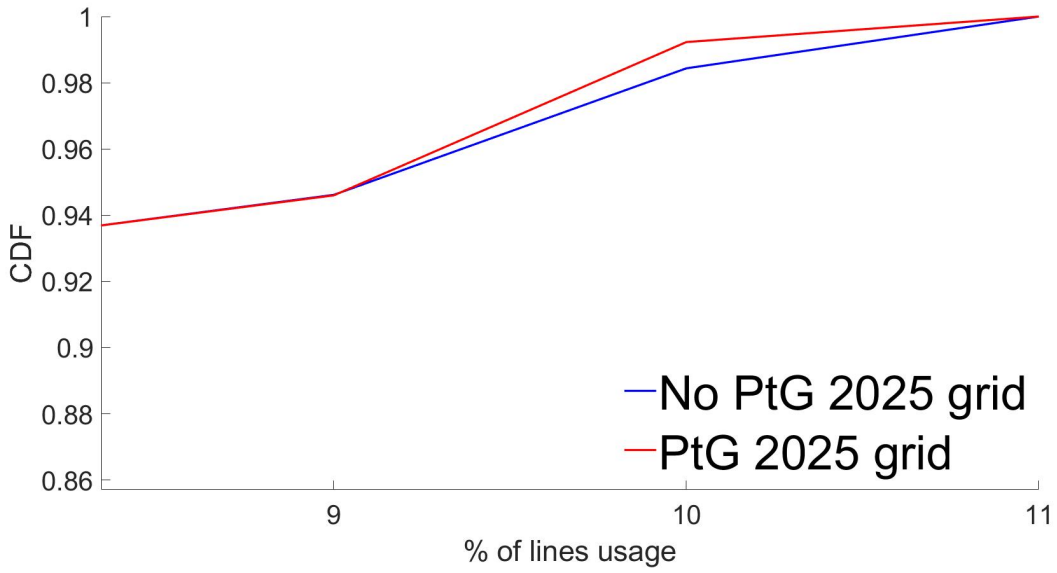

Figure 5-6. Detail of CDFs of congested lines for year 2040 in RTM simulation.

A smoother variation from saturation zone to overload area can be observed, with respect to the one occurring in the grid without PtG units, thus confirming the expectations on PtG impact on the zones in proximity of congested lines: without PtG units there is around the 3% of occurrences of lines in overload state, while this number decreases below 1% thanks to PtG effect.

Unlike the DAM framework, RES increase in RTM is subjected to a major increase.

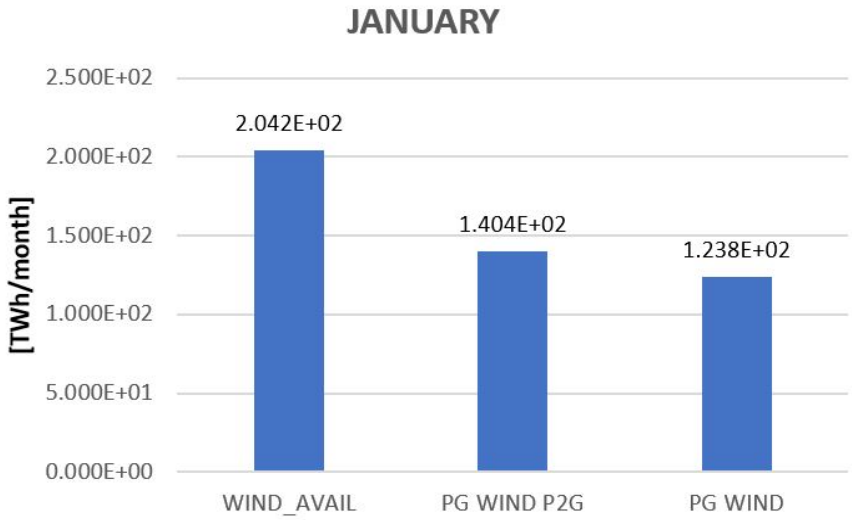

Figure 5-7. Comparison among Wind availability, Wind power produced with and without PtG in January, in RTM with 2025 grid.

The Figure 5-7 illustrates a growth of 13.5% in the wind power dispatch thanks to PtG, in January 2040 with the 2025 grid, leading to the exploitation of 68.8% of wind potential.

A stronger increase with respect to DA results is registered also in the outcomes of April simulations as showed by figure 5-8.

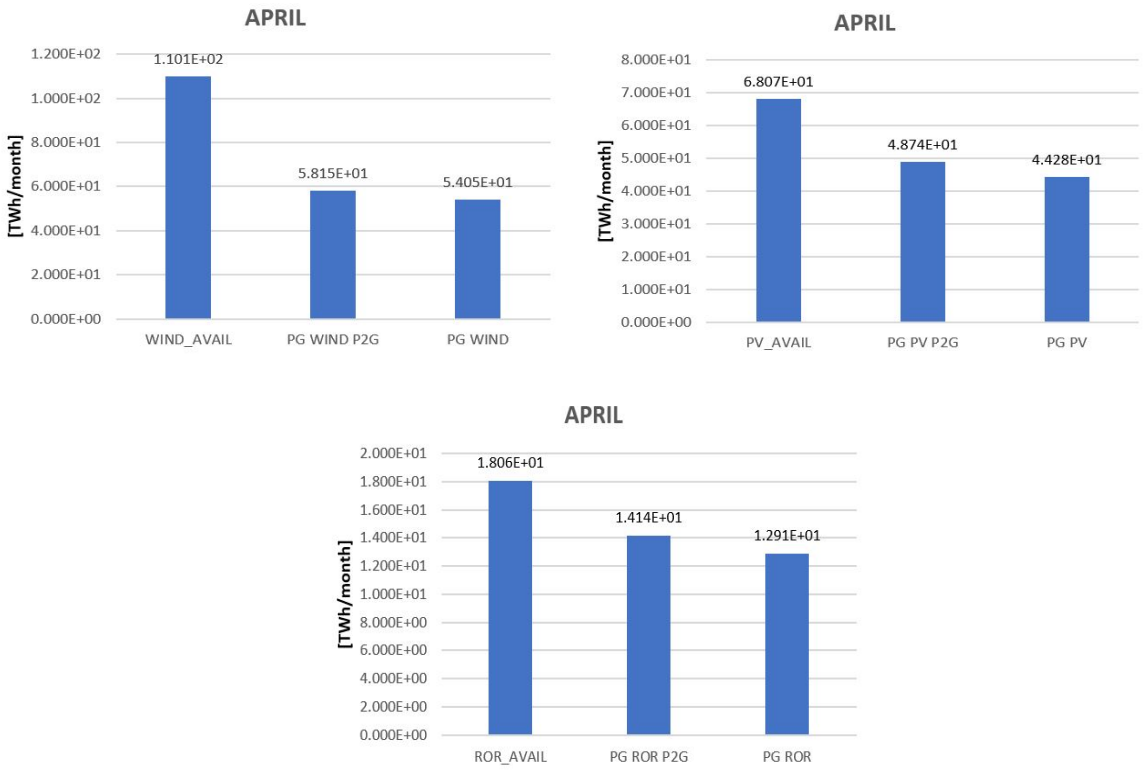

Figure 5-8. Comparison among dispatched power with PtG enabled and disabled in April 2040 scenario within RTM with 2025 grid.

Wind generation grows of the 10%, ROR generation increases of 9.6%, while PV generation has the smallest variation with only the 7.6% of growth. Results are more than doubled with respect to DA conditions.

July values confirm the expectations with an increase in PV, wind and ROR power production of 10%, 14% and 11% respectively as indicated in figure 5-9.

Figure 5-9. Comparison among dispatched power with PtG enabled and disabled in July 2040 scenario within RTM with 2025 grid.

Conversely, in October total RES production increase is limited to just 4%, showing an opposite trend with respect to other months, but still better than DA's one.

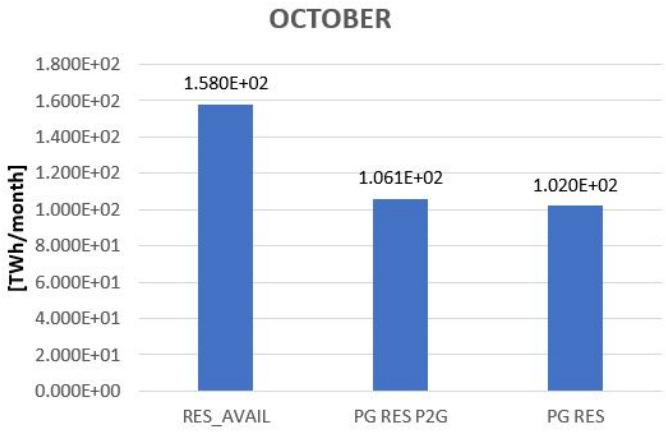

Figure 5-10. Comparison among dispatched power with PtG enabled and disabled in July 2040 scenario within RTM.

5.3.3 2040 grid simulations

To assess the effective impact of the PtG technologies it is important to perform a comparison with the benefits provided by network enhancement: infrastructural investments planned for 2040 are considered. The simulations have been carried out with the same scenario, 2040 GCA, but without the implementation of PtG. This grid contains of course a higher number of branches, thus the number of elements within the classes grows as well, although comparison not being affected due to the normalisation to the total number of elements: results are hence comparable. Comparison is always referred to the 2025 grid with PtG enabled.

5.3.3.1 DAM simulations in 2040 grid

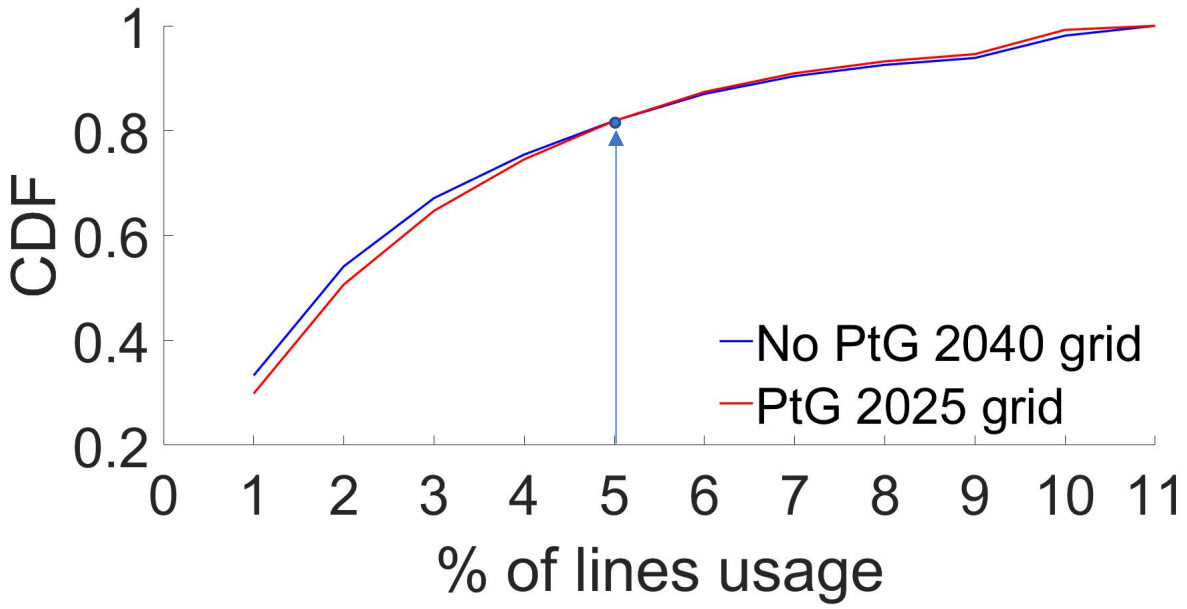

Figure 5-11. CDFs comparison between 2040 grid curve and 2025 grid curve with PtG enabled.

The Fig. 5-11 clearly describes the effects of the two types of improvement measures onto network operation: it is possible to detect a crossover point that corresponds to the 50% class, i.e. half of the capacity of the lines. Below this point it is highlighted the prevalence of the effects of the investments over the benefits provided by PtG plants, as a matter of fact they increase low loaded lines performances, that is a greater number of lines working under the half of their capacity because of the higher rating values. On the contrary at high load there are more lines congested.

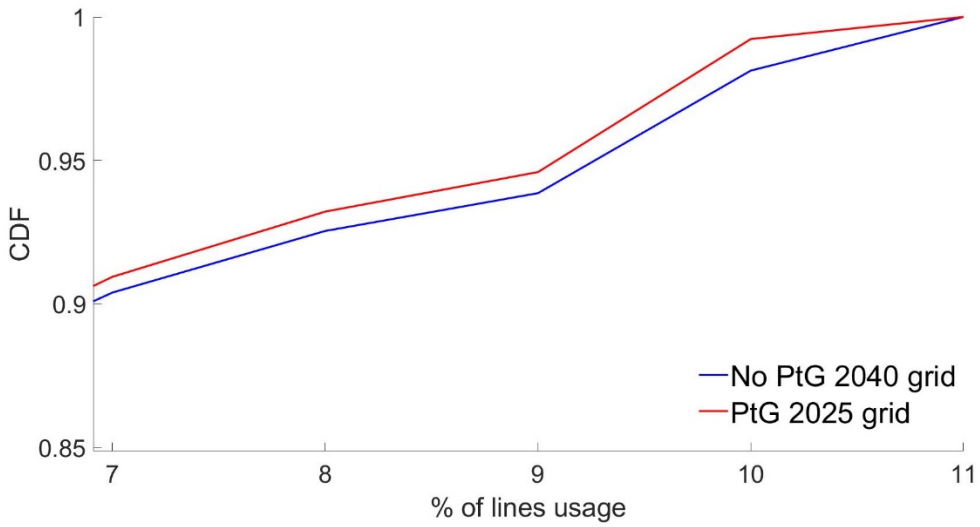

Figure 5-12. Detail of CDFs comparison between 2040 grid curve and 2025 grid curve with PtG enabled.

It is possible to observe this effect by zooming in the figure to obtain a clearer insight: less than 1% of the points are contained in the overloaded class, in the grid with PtG; while there are more than double (~ 2%) occurrences of congestion in the 2040 grid, despite a way greater capacity: that is because the strategic installation of PtG plants draws power from the surrounding congested lines, relieving the overload.

As regards RES production, it is possible to notice that available RES surplus exploited is around 3% during all the year.

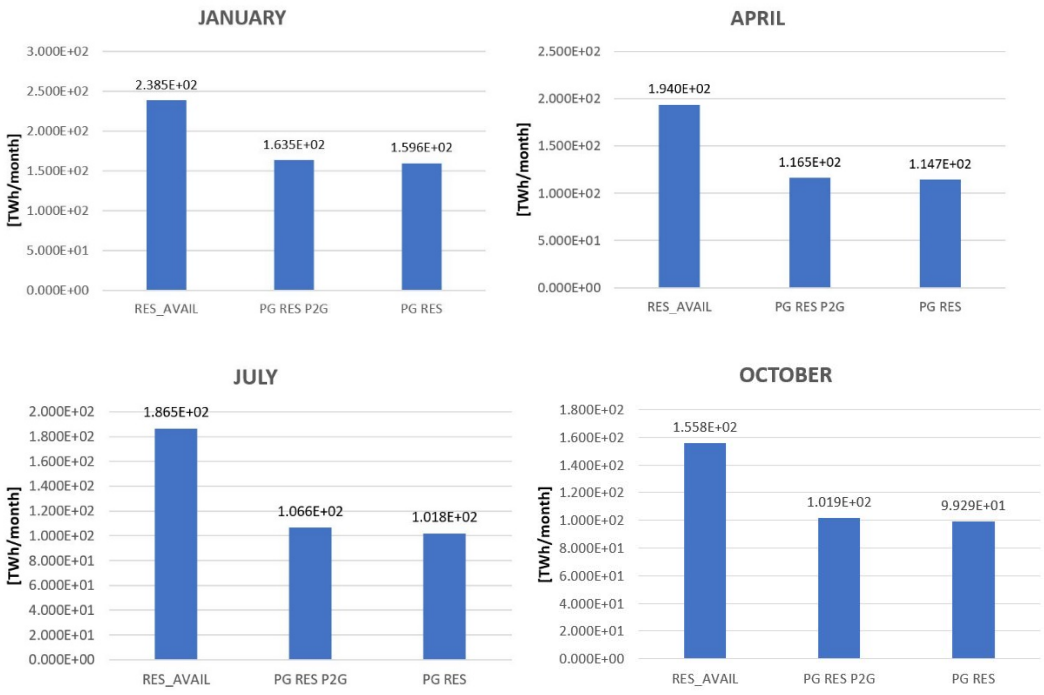

Figure 5-13. Comparison of RES production for year 2040 in the 2040 grid.

5.3.3.2 2040 RTM simulation in 2040 grid

Real time simulations on the 2040 grid have been performed under the same conditions as on the 2025 grid: maximum PtG power profile, same generation and load scenario.

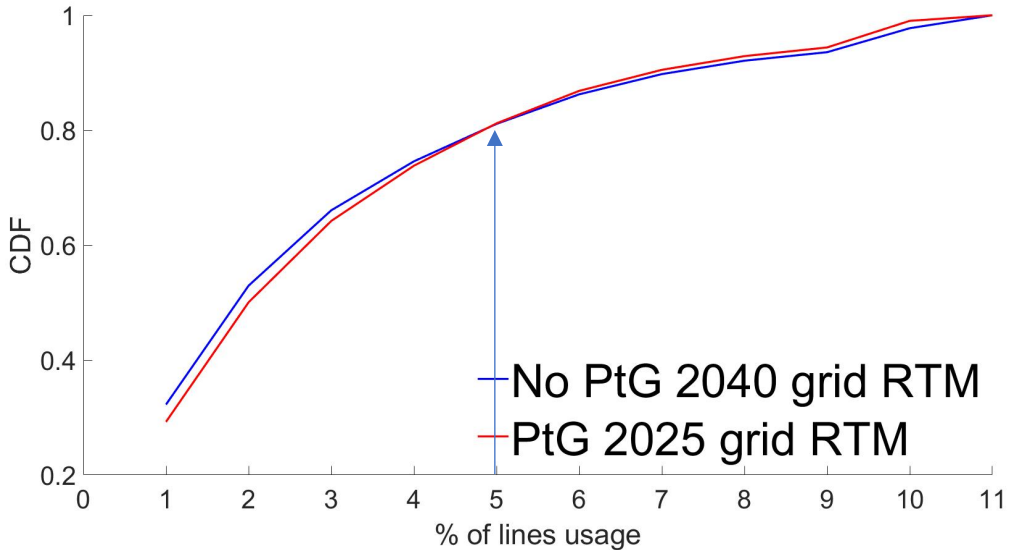

Figure 5-14 CDFs comparison between 2040 grid curve and 2025 grid curve with PtG enabled in RTM simulation.

The phenomenon observed in figure 5-14 is analogous to the one described in fig. 5-11 except for PtG effect being amplified at high load operation.

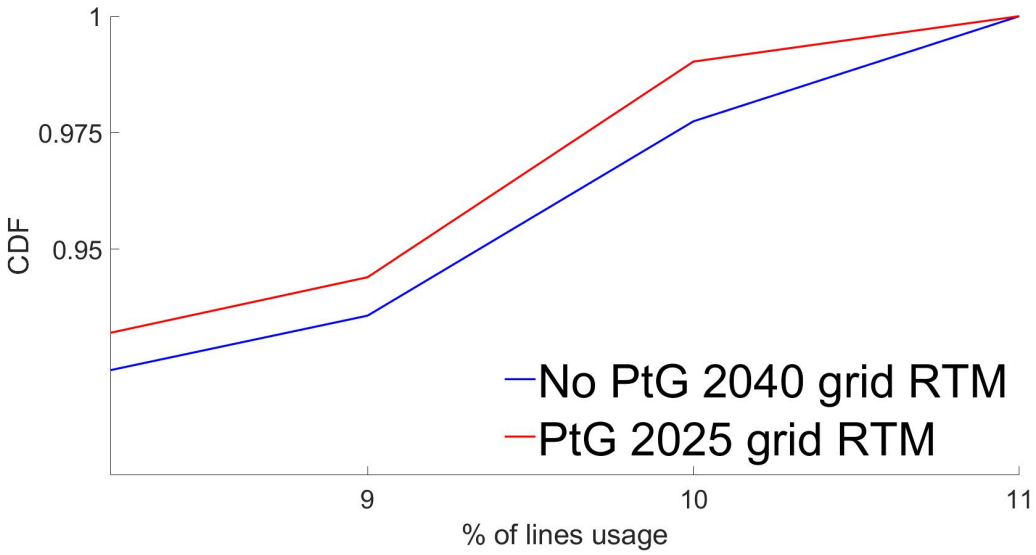

Figure 5-15. Detail of CDFs comparison between 2040 grid curve and 2025 grid curve with PtG enabled in RTM.

As a matter of fact, less than 1% of the occurrences are contained in the overload class with the PtG effect, with an improvement with respect to the enhanced grid of the 68%, representing an increase of 11% from the value obtained in DAM.

Finally, RES surplus exploitation is addressed as well, with a real time analysis. It is possible to illustrate that on certain months there is a relatively significant increase in RES dispatch, while in others PtG worsens the situation.

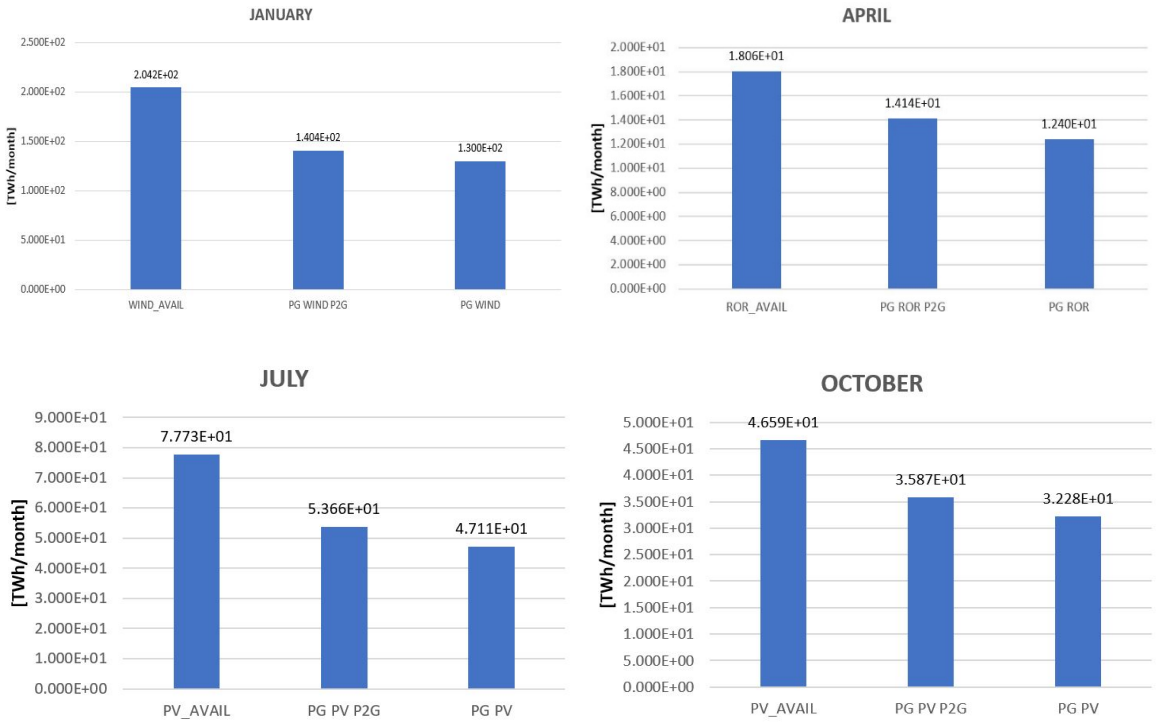

Figure 5-16. Comparison of RES production for year 2040 in the 2040 grid, in RTM.

A meaningful perspective of RES trend all over the year is given by fig. 5-16, indicating the best renewable behaviour per month. PV presents a +14% in July, where production is at its yearly peak and a +11% in October, hydro electric production from run on river plants marks a +14% in April, while wind scores a +8% in January, both being at their yearly peak as well.

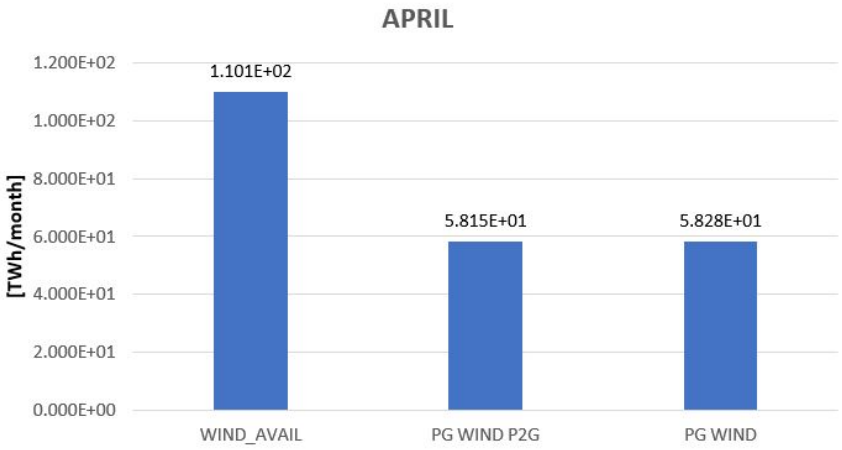

Figure 5-17. Comparison of wind production in April 2040, in the 2040 grid, RTM.

It is interesting to discuss the results presented in fig. 5-17, since they introduce a valuable consideration on PtG impact. It is possible to notice that PtG causes a decrease in wind production, in the same month when other renewables recorded a significant increase in

dispatch. This effect is deeply related to the PtG units placement: an unfortunate positioning is likely to cause worsening in both congestion relief and RES dispatch. A direct consequence of this fact, sustained by all the other results presented, is the decoupling of the two phenomena, that can occur separately and are thus not linked, except for their dependency on siting accuracy.

6 Conclusions

From the analysis of results it can be inferred that, since improvements in both congestion relief and RES dispatch are of little entity, the amount of PtG installed is not sufficient to maximize the economic return on the investments for this technology, although the effects being globally positive in almost all the cases presented. To obtain more significant benefits, the quantity of PtG installed power should be at least doubled: as a matter of fact, 16.8 GW barely represents the 0.33% of the average daily RES power available for the EU grid and the 0.17% of the average daily loads demand. Nonetheless, given the percentage of PtG penetration considered within the clustered ENTSO-E network, the results obtained can be considered valuable. For future developments it can be claimed that the outcomes of this thesis could be further improved by performing an optimization on the PtG units positioning process. In fact, the approach adopted has led to valid though not optimal results: the preliminary placement by ranking suffers the results of the power flows studies, that could not confirm the accuracy of the sites chosen; whilst, an evolutionary programming approach could serve the purpose. Assuming that the capital expenditure set in this study, i.e. 16 billion euros, may represent a constraint on the economic viability of the large-scale deployment of this technology, it is convenient to highlight the cost reduction expected for different PtG variants in table 3-4, looking in particular at the 2050 expected cost for 100 MW units. By considering an average cost of 66 million euros, the installable power rises up to 24 GW. Thus, if PtG is properly fostered by future energy plans, it can be expected a further reduction in costs that could propose PtG technology as a valid solution for both distributed storage and sustainable green gas production.

Finally, it is possible to state that though the enhancement of the network being necessary in order to sustain future power demand, withstand RES variation and power perturbances, investing and financing the system upgrade for facing the total peak power (i.e. the maximum amount of electricity that can be traded) might be needlessly expensive, due to the fact that load and RES peaks tend to occur for very limited time intervals during the year. As a consequence, PtG could be adopted on a large scale to support the network ancillary services in dealing with these events.

Appendix A – Table/List of Symbols

P - active power

Q – reactive power

$\boldsymbol{\delta}$ – voltage phase angle

k, i – nodes of the network

X_{ki} – line reactance

R_{ki} – line resistance

n – number of nodes of the network

N – set of nodes

m – number of generators

M – set of generators

p – vector of power injections

B – admittance matrix

$\mathbf{C_f}, \mathbf{C_t}$ – sparse connection matrices

References

[1] ENTSO-E, Home page, https://www.entsoe.eu/Pages/default.aspx (on line on 8th March 2018)

[2] ENTSO-E, TYNDP, http://tyndp.entsoe.eu/maps-data/ (on line on 17th July 2018)

[3] A. Mazza, E. Bompard, and G. Chicco, Applications of power to gas technologies in emerging electrical systems, Renewable and Sustainable Energy Reviews, vol.92, pp. 794-806, 2018

[4] ENTSO-E, Ten Years Network Development Plan 2016: Grid data, https://docstore.entsoe.eu/stum/, (on line 18th July 2018)

[5] J. Hörsch, F. Neumann and T. Brown, Python for Power System Analysis (PyPSA), Model of the European Energy System, https://github.com/PyPSA/pypsa-eur

[6] J. Hörsch, F. Hofmann, D. Schlachtberger, and T. Brown, Supplementary Data: Code, Input Data and Model data: PyPSA-Eur: An Open Optimisation Model of the European Transmission System, https://zenodo.org/record/1246852#.W307ay1aY_V (on line 19th July 2018)

[7] ENTSO-E, Power Statisics - Load, https://www.entsoe.eu/data/power-stats/hourly_load/ (on line on 17th July 2018)

[8] ENTSO-E, European Grid Map, https://www.entsoe.eu/data/map/ (on line on 17th July 2018)

[9] Bright Solar Resource Model, http://jamiembright.github.io/BrightSolarModel/, (online 18th July 2018)

[10] MATLAB,*k-means algorithm*, https://www.mathworks.com/help/stats/kmeans.html (on line 24th October 2018)

[11] ENTSO-E, Power Statisics - Generation, https://www.entsoe.eu/data/power-stats/net-gen-capacity/ (on line on 17th July 2018)

[12] R. D. Zimmerman, C. E. Murillo-Sanchez, and R. J. Thomas, Matpower: Steady-

State Operations, Planning and Analysis Tools for Power Systems Research and Education, IEEE Transactions on Power Systems, vol. 26, pp. 12-19, Feb. 2011 http://dx.doi.org/10.1109/TPWRS.2010.2051168

[13] J. Hörsch, F. Hofmann, D. Schlachtberger, and T. Brown, PyPSA-Eur: An Open Optimisation Model of the European Transmission System, Preprint submitted to International Journal of Energy Strategy Reviews, June 2018, https://arxiv.org/pdf/1806.01613.pdf

[14] J.M. Bright, C.J. Smith, P.G. Taylor, and R. Crook, “Stochastic generation of synthetic minutely irradiance time series derived from mean hourly weather observation data”, Solar Energy, vol. 115, pp. 229-242, 2015, DOI: http://dx.doi.org/10.1016/j.solener.2015.02.032

[15] A.Mazza, E.Carpaneto, G.Chicco, and A.Ciocia, Creation of Network Case Studies With High Penetration of Distributed Energy Resources, UPEC 2018, Glasgow, 4th-7th September 2018

[16] Mercato Elettrico, GME https://www.mercatoelettrico.org/it/Mercati/MercatoElettrico/MPE.aspx

[17] EPRI, Wholesale electricity market design initiatives in the United States: Survey and research needs, Electric Power Research Institute, 2016 Technical Update

[18] www.geojson.io website used to visualize the map in figure 2.1.

[19] A.J. Wood, B.F. Wollenberg, Power Generation, Operation and Control, John Wiley & Sons,Inc. 1996.

[20] A. Rogin, Computational framework for evaluating the impact of power-to-gas technology on European transmission system with large penetration of renewable sources, 2018.

[21] https://www.mercatoelettrico.org/En/Mercati/MercatoElettrico

[22] C. E. Murillo-Sanchez, R. D. Zimmerman, C. L. Anderson, and R. J. Thomas, “Secure Planning and Operations of Systems with Stochastic Sources, Energy Storage and Active Demand,” Smart Grid, IEEE Transactions on, vol. 4, no. 4, pp. 2220–2229, Dec. 2013, http://dx.doi.org/10.1109/TSG.2013.2281001. 1, 1.2, 3

[23] E. Bompard, S. Bensaid, G. Chicco, A. Mazza, F. Salomone, D6.4 Report on the model of the power system with PtG, Oct. 2018.

[24] https://tyndp.entsoe.eu/tyndp2018/projects/projects

[25] 2nd ENTSO-E Guideline For Cost Benefit Analysis of Grid Development Projects p29, Sept. 2018 https://docstore.entsoe.eu/Documents/TYNDP%20documents/Cost%20Benefit%20Analysis/2018-10-11-tyndp-cba-20.pdf

[26] J.Schaffert, H. Cigarida, M. Lange, D. Levedag, D. Coquette. D8.7, Report on data and methods used for the potential analysis of power-to-methane in Europe”, Apr 2019.

[27] Improvements of TYNDP 2018, ENTSO-E, 2018. https://tyndp.entsoe.eu/Documents/TYNDP%20documents/TYNDP2018/consultation/Communication/ENTSO_TYNDP_2018_Improvements.pdf

[28] Report on Unit Investment Cost Indicator and Corresponding Reference values for Electricity and Gas Infrastructure, ACER, 2015.
http://www.acer.europa.eu/Official_documents/Publications/UIC_Electricity_History/UIC%20Report%20%20-%20Electricity%20infrastructure.pdf

[29] https://tyndp.entsoe.eu/tyndp2018/

[30] Scenario Report TYNDP 2018, ENTSO-E
https://docstore.entsoe.eu/Documents/TYNDP%20documents/TYNDP2018/Scenario_Report_2018_Final.pdf

[31] Annex II Report, ENTSOG, ENTSO-E, 2017.

[32] J.Gorre, C. van Leeuwen, F. Ortloff. D8.6 Report on the optimal time profile and operation of the conversion technology during a representative year, in the perspective of the available storage capacities, 2018

[33] European Commission, European Meteorological derived high resolution renewable energy source generation time series, https://ec.europa.eu/jrc/en/scientific-tool/emhires (on line 18th July 2018)

[34] C. E. Murillo-S´anchez, R. D. Zimmerman, C. L. Anderson, and R. J. Thomas, “Secure Planning and Operations of Systems with Stochastic Sources, Energy Storage and Active Demand,” Smart Grid, IEEE Transactions on, vol. 4, no. 4, pp. 2220–2229, Dec. 2013, http://dx.doi.org/10.1109/TSG.2013.2281001.

[35] European Pollutant Release and Transfer Register https://prtr.eea.europa.eu/#/home

[36] M.Mitchell. “An Introduction to Genetic Algorithms”. Cambridge, 1996.

[37] “Electric Power Distribution and Utilization - Distribution System Planning”, Gianfranco Chicco 2014

[38] https://www.genscape.com/blog/stay-ahead-congestion-caused-surplus-renewables